JVI Accepted Manuscript Posted Online 6 December 2017
J. Virol. doi:10.1128/JVI.00941-17

Title: Characterization of an influenza virus pseudotyped with Ebolavirus glycoprotein

Julie Xiao,[a] Pramila Rijal,[a] Lisa Schimanski,[a] Arun Kumar Tharkeshwar,[b*] Edward Wright,[c] Wim Annaert,[b] Alain Townsend[a#]

Human Immunology Unit, Weatherall Institute of Molecular Medicine, Oxford, United Kingdom[a]

VIB-Center for Brain and Disease Research, Laboratory for Membrane Trafficking, Leuven, Belgium & KU Leuven, Department of Neurosciences, Leuven, Belgium[b]

Viral Pseudotype Unit, Faculty of Science and Technology, University of Westminster, London, United Kingdom[c]

[#]Address correspondence to Alain R. M. Townsend, alain.townsend@imm.ox.ac.uk.

*Present address: Arun Kumar Tharkeshwar, Yale School of Medicine, Department of Cell Biology, 333 Cedar Street, New Haven, CT

Word count for the abstract: 231; for “importance”: 143

Word count for the text: 5811

Abstract

We have produced a new Ebola virus pseudotype: E-S-FLU, which can be handled in biosafety level-1/2 containment for laboratory analysis. E-S-FLU is a single cycle influenza virus coated with Ebolavirus glycoprotein, and it encodes enhanced green fluorescence protein as a reporter that replaces the influenza haemagglutinin. MDCK-SIAT1 cells were transduced to express Ebolavirus glycoprotein as a stable transmembrane protein for E-S-FLU production. Infection of cells by E-S-FLU was dependent on Niemann-Pick C1 protein, which is the well-characterized receptor for Ebola virus entry at the late endosome/lysosome membrane. E-S-FLU was neutralized specifically by anti-Ebola glycoprotein antibody and a variety of small drug molecules that are known to inhibit entry of wild-type Ebola virus. To demonstrate the application of this new Ebola virus pseudotype, we show that a single laboratory batch was sufficient to screen a library (LOPAC®1280 Sigma) of 1280 pharmacologically active compounds for inhibition of virus entry. 215 compounds inhibited E-S-FLU infection, while only 22 inhibited the control H5-S-FLU virus coated in an H5 haemagglutinin. These inhibitory compounds have very dispersed targets and mechanisms of action e.g. calcium channel blockers, estrogen receptor antagonists, anti-histamines, serotonin uptake inhibitors etc. and this correlates with inhibitor screening results with other pseudotypes or wild-type Ebola virus in the literature. E-S-FLU is a new tool for Ebola virus cell entry studies and is easily applied to high throughput screening assays for small molecule inhibitors or antibodies.

Importance

Ebola virus is from the *Filoviridae* family and is a biosafety level 4 pathogen. There are no FDA-approved therapeutics for Ebola virus. These characteristics warrant the development of surrogates of Ebola virus that can be handled in more convenient laboratory containment to study the biology of the virus, and screen for inhibitors. Here we characterized a new surrogate named E-S-FLU, that is based on a disabled influenza virus core coated with the Ebola virus surface protein, but does not contain any genetic information from the Ebola virus itself. We show that E-S-FLU uses the same cell entry pathway as wild-type Ebola virus. As an example of the ease of use of E-S-FLU in biosafety level-1/2 containment, we showed that a single production batch could provide enough surrogate virus to screen a standard small molecule library of 1280 candidates for inhibitors of viral entry.

Introduction

Ebola virus is a filamentous RNA virus that belongs to the *Filoviridae* family (1). It has a negatively stranded RNA genome (19kb) that encodes 7 genes. Ebola virus is a zoonotic virus and the mechanism by which is it maintained in its natural reservoirs such as fruit bats is not fully understood (2). The first Ebola outbreak in the human population happened in Congo and Sudan in 1976. During the Ebola outbreak, *Zaire* ebolavirus was first isolated and characterized (3, 4). Since then, five species of ebolavirus have been identified: *Zaire*, *Sudan*, *Taï Forest*, *Bundibugyo* and *Reston* (5). Ebola virus is highly infectious in human and non-human primates, and causes a haemorrhagic fever with a fatality rate of 25-90% (1). The recent epidemic in 2014-2015 caused nearly 30,000 human infections and more than 11,000 deaths in West Africa (World health organization, March 2016). So far, there is no FDA-approved treatment or vaccine against Ebola virus disease, but the recombinant VSV-GP vaccine has shown very promising protection in the Guinea ring vaccination trial (6).

Although much attention has been drawn to Ebola virus research since then, direct handling of Ebola virus is limited to biosafety level 4 laboratories. Development of a safe substitute is very important and useful for high-throughput screening of therapeutics, diagnostic screening of neutralizing human sera, and understanding the entry mechanism of Ebola virus.

Ebola virus is a lipid-enveloped virus, and the glycoprotein (EBOV-GP) is the only protein presented at the virus surface. EBOV-GP plays an important role in virus cell entry, and it is the key target for neutralisation by antibodies (7). Currently available viral surrogates for EBOV, such as EBOV-GP pseudotyped lentivirus (8) and vesicular stomatitis virus (VSV) (9), expose EBOV-GP at the viral surface. However, EBOV-GP pseudotyped viruses are still different from wild-type Ebola virus, and vary in their biological properties and susceptibility to neutralizing antibodies. Recently the National Institute of Biological Standards and Control (NIBSC) has compared 22 different Ebola-based *in vitro* assays with the wild-type Ebola virus for neutralization by a panel of antibodies and sera. The results showed variable but generally poor correlations (10). Therefore, designing and comparing additional EBOV-GP pseudotyped viruses is important to accurately determine the correlates of protection.

Here we describe a new Ebola virus pseudotype (E-S-FLU) based on a non-replicating influenza virus S-FLU (11). Influenza virus is also a negatively stranded RNA virus. S-FLU has its haemagglutinin gene replaced by an enhanced green fluorescence protein (eGFP) reporter. We found that unlike other cell lines (12–19), MDCK-SIAT1 can stably express high levels of EBOV-GP without apparent toxicity. Pseudotyping is done by simply infecting MDCK-SIAT1 producer cell lines (20) that are stably transduced to express EBOV-GP, with seed S-FLU virus. The expression of the EBOV-GP in the producer cell line complements the defect in haemagglutinin expression, and the S-FLU replicates to levels sufficient to perform drug inhibition or antibody neutralization assays without further concentration. The stable producer cell line allows easy production of E-S-FLU without the need of repeated transfection for each round of virus production, in comparison to lentivirus pseudotyping and VSV psueodypting methods. E-S-FLU does not contain any genetic materials from the Ebola virus and can infect cell lines that do not express EBOV GP or influenza HA for only a single cycle. Therefore, it can be handled at biosafety level 1/2. We have shown that E-S-FLU is easy to produce, and it resembles Ebola virus during the cell entry process. We also compared E-S-FLU with recombinant wild-type Ebola virus in drug screening assays, and the results were highly correlated. E-S-FLU is a useful surrogate for Ebola virus *in vitro* studies.

Results

Generation of EBOV-GP pseudotyped S-FLU

S-FLU is a pseudotyped influenza virus with its endogenous haemagglutinin sequence removed, and it was previously pseudotyped with different subtypes of influenza haemagglutinin (11, 21). In order to incorporate EBOV-GP in the S-FLU envelope, we used a lentiviral vector to transduce MDCK-SIAT1 cells to express full length Zaire strain EBOV-GP gene (*Zaire* wt/GIN/2014/ Kissidougou-C15). Transduced cells were healthy in morphology (Fig. 1). EBOV-GP was expressed at the cell surface and can be detected by GP-specific monoclonal antibody KZ52. Cells with high expression of EBOV-GP were sorted and stored as the E-SIAT cell line. GP surface expression was not toxic to MDCK-SIAT1 cells, and the expression is stable and uniform up to at least the ninth passage (Fig. 1).

Cloned seed S-FLU virus that is coated in influenza haemagglutinin (HA) was added to propagate in E-SIAT cells to produce EBOV-GP pseudotyped S-FLU. After 48 hours culture supernatants were harvested and titrated on indicator MDCK-SIAT1 cells for infection. Infected MDCK-SIAT1 cells express eGFP that is encoded in the virus. We named the new pseudotype E-S-FLU. E-S-FLU reaches a lower titer compared to viruses grown in the H5 HA transduced producer cells and forms small diffuse plaques compared to H5-S-FLU (Fig. 2C) (21). Typical EC50 dilutions for E-S-FLU at 48 hours were ~1:8 compared to ~1:500 for H5-S-FLU (Fig. 2A). From the EC50 dilution, and the number of cells per well ($3x10^4$), the Cell Infectious Dose 50% (CID50/ml) in the E-S-FLU batch was calculated as ~$2X10^6$ CID50/ml, H5 S-FLU as ~$1.6x10^8$ CID50/ml. However, the harvested culture supernatant from E-SIAT cells contains adequate pseudovirions for 50 µl of a 1:4 dilution to give close to full infection of the $3x10^4$ cells in a well of a 96-well plate. No further purification or concentration steps are needed for screening inhibitory drugs or antibodies. With the same protocol, we were also able to pseudotype S-FLU with Bundibugyo, Sudan and Mayinga-Zaire EBOV-GP to similar viral titers (data not shown).

It has been shown in the literature that the transmembrane and cytoplasmic domain of Influenza HA is important for flu viral particle assembly (22-29). To potentially improve the viral titer of E-S-FLU, we designed a GP-HA hybrid protein, which contains the extracellular domain of the EBOV-GP and the transmembrane and cytoplasmic domain of HA. After transduction and sorting, GP-HA protein can be detected by antibody KZ52 at the surface of EH-SIAT cells at the similar level as the E-SIAT cells. However, to our surprise, no infective S-FLU was detected from the EH-SIAT cell supernatant (data not shown).

E-S-FLU infection requires NPC1 as receptor

NPC1 protein has been identified as the key entry receptor for Ebola virus at the level of late endosome/ lysosome membrane (30-32). We infected both wild-type HeLa cells and two NPC1 knockout HeLa cell lines (ex2 NPC1-KO and ex4 NPC1-KO) (33) using E-S-FLU and H5-S-FLU (Fig. 3). Wild-type HeLa cells were infected by E-S-FLU and expressed eGFP. E-S-FLU infection was completely blocked in NPC1-KO cells. In contrast, percentage infection by H5-S-FLU were the same for wild-type and NPC1-KO cells. This shows that E-S-FLU requires NPC1 for cell entry, which resembles the wild-type Ebola virus cell entry mechanism.

E-S-FLU is specifically neutralized by EBOV-GP antibody

To further validate our new EBOV-GP pseudotyped E-S-FLU, we tested it in the antibody micro-neutralization assay in comparison to control pseudotype H5-S-FLU and EBOV-GP coated lentivirus pseudotype (GP-lentivirus). H5-S-FLU contains exactly the same S-FLU core as E-S-FLU but differs at the surface glycoprotein. GP-lenti is a lentivirus pseudotyped with the full length Zaire-strain EBOV-GP (wt/GIN/2014/Kissidougou-C15), matched to E-S-FLU.

Neutralization profiles for two antibodies are shown in Fig. 4. KZ52 is a human monoclonal antibody that specifically binds to *Zaire* species of EBOV-GP, and recognizes a conformational epitope at the base of GP (34, 35). KZ52 neutralized E-S-FLU and GP-lenti pseudotyped virus with a similar EC50 value to what has been reported on wild-type Ebola virus (300 ng/ml, (34)), while it did not neutralize H5-S-FLU. The neutralization effect was confirmed by fluorescence microscopy (Fig 4E and 4F). In contrast, 21D85A, a H5 specific monoclonal antibody, neutralized H5-S-FLU but did not neutralize E-S-FLU or GP-lenti pseudotyped virus. This shows that the E-S-FLU pseudotyped virus we produced is coated with correctly folded EBOV-GP, and requires this molecule to infect the MDCK-SIAT1 indicator cells. These results show that E-S-FLU can be used to screen for neutralizing antibodies to Ebola virus.

Inhibition of E-S-FLU infection by small molecules

In the literature, several drug screen studies have been done with wild-type Ebola virus (36-40) and Ebola virus surrogates such as Ebola viral like particles (41), EBOV-GP pseudotyped rVSV (31) and lentivirus (42, 43). It was shown that drug molecules with diverse pharmacological functions have inhibited Ebola virus infection *in vitro*. To verify the use of E-S-FLU in drug screening assays, we selected several types of drug molecules that have been tested repeatedly in the literature and screened them against E-S-FLU in our drug inhibition assay. Table 1 summarizes the 13 initial inhibitors we have tested. E-S-FLU infection was effectively blocked by different groups of drugs, and the IC50 values were in the same range as those in the literature.

All screens in Table 1 were repeated at least 3 times to calculate the geometric mean and 95% confidence interval of IC50. IC50 value is the drug concentration at which the eGFP fluorescence was reduced by 50%. We have also screened these drugs against H5-S-FLU (supplementary table S1). Most of them did not inhibit H5-S-FLU, except Niclosamide at 2.64μM. Fig. 5 shows an example of drug inhibition by Tetrandrine. Infection level was quantified by eGFP expression. We also estimated the toxicity for each drug by staining the cells with fluorescently labelled-wheat germ agglutinin (WGA) after infection, fixation and wash. WGA is a lectin that binds to cell surface N-acetyl-D-glucosamine and sialic acid. Cells in good condition will remain adhered to the plate during analysis, and can be detected by WGA. Dead cells or unhealthy cells will detach and be washed away. WGA staining allows quick indication of drug toxicity in high-throughput plate screening assays. This is verified by light microscopy (Fig. 5C and 5D).

We have shown the calculated logP and pKa values of these inhibitors in Table 1. As found by others, many of the drug molecules that inhibited Ebola virus have high logP and high pKa values (e.g. Amiodarone, Verapamil, Clomiphene) and can be classified as cationic amphipathic drugs (36, 44). There are also non-cationic amphiphiles that inhibited Ebola virus entry, such as EIPA: 5-(N-Ethyl-N-isopropyl Amiloride (45) and MDL28170 (42, 46), E64 (43, 47–49) and Niclosamide (41). The potential mode of action of each of these molecules is shown in Fig. 8.

LOPAC®1280 library screen

Having established that infection by E-S-FLU was dependent on NPC1 receptor, and was inhibited by specific antibodies and established small molecules, we proceeded to a formal drug screen. We have screened 1280 drug molecules from the LOPAC®1280 library (Sigma-Aldrich) in our drug inhibition assay to test their effect on E-S-FLU and H5-S-FLU infection. This library contains 1280 pharmacologically active small molecules with different molecular targets. All drugs were screened in the first round at 100 μM and 5 μM. Selected drugs were then titrated once in drug inhibition assay to calculate their IC50.

In total, 215 out of 1280 molecules inhibited E-S-FLU infection to some level before reaching their toxicity *in vitro* (Fig. 6, 7 and supplementary table S1). Out of the 215 that inhibited E-S-FLU, 58 had an IC50 of less than 10 μM. In comparison, only 22 of the 1280 molecules inhibited H5-S-FLU and 8 had IC50 of less than 10 μM. All of these 22 molecules (Table 3) also inhibited E-S-FLU, and thus were likely to be acting either on both EBOV-GP and Influenza HA, or at a post entry stage that is independent of the surface glycoprotein. We did not see any molecule that inhibited H5-S-FLU but did not inhibit E-S-FLU. The detailed profile for all the inhibitors is shown in the supplementary table S1. These 215 inhibitors come from a variety of pharmacological groups according to the description on Sigma's website (Fig. 6). The table S1 also includes 13 small molecules tested in addition to the LOPAC1280 library to give a total of 228 inhibitors of E-S-FLU and of these, 25 that inhibited both E-S-FLU and H5-S-FLU (Fig. 7, Table 3).

In our screening system, we quantified infection by measuring the overall fluorescence level of cells. Under the fluorescence microscope, it was clear that most drugs reduced the number of fluorescent cells (i.e. reduced the proportion of infected cells) as the drug concentration increased. 12 drugs however, caused a reduced overall fluorescence level of infected cells without reducing the number of fluorescent cells significantly. All these 12 drugs also affected H5-S-FLU infection. This suggests that they acted at a post entry phase, by limiting the expression of viral proteins. In Table 3, they are annotated as the "dimmer" drugs. The other 13 molecules that inhibited both E-S-FLU and H5-S-FLU reduced the number of infected cells, and thus may have affected the function of both glycoproteins.

The IC50 of all 228 molecules that have inhibited E-S-FLU were plotted in Fig. 7. These include the 215 inhibitors from the LOPAC®1280 library together with the additional 13 individual drugs we have tested in addition to this library.

Comparison with Johansen et al., screen

We compared our screening results with a recently published drug screening paper from Johansen et al., (39), in which wild-type EBOV was used to screen for inhibitors. There are 538 drugs in common between the two libraries (Table 2). 442 had agreed results; out of which 23 drugs were inhibitors and 419 showed no effect. For the rest of the drugs, 70 were positive in LOPAC®1280 screen only, and 26 were positive in Johansen's screen only. We performed a two-tailed Fisher's exact statistical analysis on the comparison, and the correlation is significant (P value < 0.0001).

One of the main differences between the two screens is the range of drug concentration being tested. The highest concentration tested in the Johansen's screen was 13 μM whereas in our screen most drugs have been screened with concentrations higher than 50μM if toxicity is not reached. For this reason, the great majority of "agreements" occurred in the drugs with IC50 less than 10μM in our assay (Table S1). For the drugs that were positive in LOPAC®1280 screen only, we selected Ebastine (E9531), Imipramine (I7379), Verapamil (V4629) and ordered them individually from Sigma to confirm their inhibitory effect. All three drugs showed the inhibitory effect on E-S-FLU with comparable IC50 as the LOPAC®1280 library screen. All 3 drugs have been reported as inhibitors in other papers (31, 36, 41).

From the 26 drugs that were positive in Johansen's screen but negative in our LOPAC1280 screen, we have ordered individually from Sigma and further tested 14 drugs: Auranofin (Sigma code: A6733), Bepridil (B5016), Calcimycin (C7522), D609 (T8543), Diphenyleneiodonium (D2926), Doxylamine (D3775), Linezolid (PZ0014), Naproxen (M1275), Nocodazole (M1404), Perphenazine (P6402), Rotenone (R8875), Sanguinarine (S5890), Serotonin (H9523) and Thapsigargin (T9033).

Bepridil (a calcium channel inhibitor) and Perphenazine (a cationic amphiphile) from the LOPAC®1280 library did not inhibit E-S-FLU, but the individually ordered samples showed specific inhibition to E-S-FLU (Bepridil IC50=2.7 µM, Perphenazine IC50=8.2 µM). This indicates some variation due to false negatives in the library preparation from Sigma.

D609, Doxylamine, Disopyramide, Linezolid, Naproxen, Rotenone and Sanguinarine were confirmed as non-inhibitors for E-S-FLU in our assay up to 100 µM. Auranofin, Calcimycin, Diphenyleneiodonium, Nocodazole and Thapsigargin were toxic to MDCK-SIAT1 cells even at 0.2 µM, yet some cells were still infected. None of the drugs that are further tested inhibited H5-S-FLU.

Discussion

The design of E-S-FLU was based on a pseudotyped influenza virus, S-FLU that was previously developed in our group and is similar to other single cycle influenza pseudotypes (11, 21, 50). E-S-FLU is a non-replicating pseudotyped virus and can be manipulated at biosafety level 1/2 as it does not encode any genetic information from Ebola Virus. For ease of production we found that the MDCK-SIAT1 cell line (20) can stably express full length EBOV-GP without toxicity. Although replication of the S-FLU core in the EBOV-GP transduced cell line is 2 to 3 orders of magnitude less efficient than in the H5 HA expressing cells (Fig. 2), production of the pseudotype at a scale sufficient for high throughput assays is simple and efficient. E-S-FLU encodes eGFP as a reporter in preference to firefly luciferase, or beta-lactamase (9, 51, 52). Enzyme reporters are much more sensitive than eGFP, and very low-level infection can be amplified and detected. However, cells have to be lysed to release the enzymes, and then substrate is added for one round read-out only. In comparison, for drug inhibition and neutralization assays S-FLU can be added to indicator cells at a MOI >=1 to produce bright eGFP fluorescence in the majority of cells that is stable over months after fixation, and can be measured in a plate reader or observed in the microscope without further manipulation (Fig. 4, 5).

To validate E-S-FLU as a useful surrogate for Ebola virus, we showed that infection is fully dependent on the NPC1 receptor (Fig. 3), is inhibited by EBOV-GP specific antibody KZ52 (34, 35) (Fig. 4), and is also inhibited by a well characterized set of thirteen drugs that are thought to act at various points during viral entry (36-38, 40, 41) (Table 1, Fig. 8).

Several laboratories have observed that a wide variety of FDA-approved drugs can inhibit infection of cell lines *in vitro* by Ebola virus (39, 41). We have screened 1280 drugs from the LOPAC®1280 library to identify pharmacologically active small molecules that inhibit E-S-FLU cell entry. H5-S-FLU was tested in parallel to E-S-FLU to differentiate inhibition specific to EBOV-GP or to the S-FLU core. We identified 215 molecules from the library that inhibited E-S-FLU, whereas only 22 inhibited H5-S-FLU, all of which also inhibited E-S-FLU. Therefore the inhibitory effects of 193 drugs were EBOV-GP dependent.

We compared our screening result with the list of drugs screened by Johansen et al., (39), who screened 2635 small molecules on GFP expressing Ebola virus. 538 small molecules overlapped between the two libraries (Johansen vs. LOPAC®1280). Out of these overlaps, 442 molecules had concordant results between the two screens.

Correlation was statistically significant (P value < 0.0001). It is noteworthy that we identified at least 17 calcium channel inhibitors as specific inhibitors of E-S-FLU infection. Independent evidence exists for a possible role for calcium channels in the lysosomal membrane in viral entry (36, 37), perhaps through an effect on vesicle fusion (31, 53, 54). Recent studies suggested that two-pore channel 2 (TPC-2), a lysosomal calcium channel, is involved in the Ebola virus entry process, and this could be the target for the calcium channel inhibitors (37, 55).

A large group of inhibitors share a common cationic amphiphilic feature, i.e. a hydrophilic end, usually a weak base amine group (high pKa) and a hydrophobic end (high logP), and are therefore likely to concentrate in lysosomes (56-58). The mechanism by which these drugs inhibit Ebola virus entry is not resolved (36, 38). Some cationic amphiphilic drugs can cause an increase in cholesterol accumulation in endosome and lysosome where EBOV-GP membrane fusion occurs. Others can influence the lysosomal membrane stability and indirectly inhibit Acid Sphingomyelinase, which are also known as Functional Inhibitors of Acid Sphingomyelinase (FIASMAs) (59, 60), and may have an indirect effect on calcium mobilization from the lysosome through the accumulation of sphingosine. In addition the most powerful member of the cationic amphiphilic group, Toremifene, has been shown to bind to a hydrophobic pocket in the EBOV-GP and destabilize the molecule *in vitro* (61), and so may have two sites of action.

Many of these drugs have been identified to have a risk of causing long-QT syndrome, such as Amiodarone, Toremifene, Clarithromycin (62, 63). Inhibition of the potassium channel hERG (human ether-a-go-go) in cardiac myocytes is commonly associated with long-QT syndrome (64). After comparing the 228 drugs that inhibited E-S-FLU in our studies with the hERG screening literature (64-66), we identified at least 46 (20.2% indicated in Table S1) as confirmed inhibitors of the hERG channel and hence may have this dangerous side-effect on cardiac conduction. The majority of these hERG binders are typical Cationic Amphipathic Drugs. It is unclear whether the features that inhibit Ebola virus entry also predispose to the effect on hERG binding and lengthening of the Q-T interval. Further dissecting their mechanisms of action is therefore necessary before administering them to Ebola virus infected patients, despite the fact that they are FDA-approved drugs (67, 68). As more potential mechanisms of action of these drugs are uncovered, testing combinations that act at different sites for synergistic effects may be valuable to reduce this risk (69, 70).

One advantage of our S-FLU pseudotype is that infected cells express eGFP and fluoresce brightly. Visual inspection of cells in the assay plates by fluorescence microscopy revealed that two forms of inhibition could be distinguished. In the majority of cases the drugs reduced the number of infected cells. All of the 203 drugs that acted in an EBOV-GP dependent manner reduced the number of infected cells, which is consistent with inhibition of viral entry (Supplementary table S1). By contrast, in some cases the drugs did not reduce number of infected cells, but reduced the intensity of fluorescence expression in the infected cell population. Of the 228 drugs tested, 12 reduced fluorescence intensity (Table 3). All of these also inhibited H5-S-FLU. In general the IC50s for these agents were similar for E-S-FLU and H5-S-FLU, which is consistent with them acting on functions controlled by the influenza core, which is common to both. We suggest that they affect the virus at a post-entry level like Faviparivir, a specific inhibitor of RNA-dependent RNA polymerase (71-74), which was initially synthesized to inhibit influenza virus but later found effective against Ebola virus *in vitro*. In addition Aminopterin, a dihydrofolate reductase inhibitor; Brequinar, a dihydroorotate dehydrogenase inhibitor (75-78); and Ribavirin a guanosine analogue nucleoside inhibitor (70, 79, 80) may affect transcription indirectly by blocking the biosynthesis of nucleotides. It is interesting that spiranalactone and triamterene both have the “dimmer” effect. These drugs are used clinically as diuretics that block sodium channels. It is unclear how they can affect the functions of the influenza virus core at a post-entry level.

Of the 25 drugs that inhibited both H5-S-FLU and E-S-FLU, 13 reduced the number of infected cells, and thus may have inhibited cell entry by both H5 haemagglutinin and EBOV-GP. Of these Chloroquine (a lysomotropic drug) and Niclosamide may act by reducing the lysosmal proton concentration, which can influence the efficiency of cathepsin in endosome digesting EBOV-GP (81). Niclosamide is a proton ionophore (82, 83) and gave a similar IC50 on H5-S-FLU (3.3 μM) and E-S-FLU entry (1.7 μM). Arbidol may inhibit fusion of viral and lysosome membranes in a manner related to its effect on influenza haemagglutinin (84-86). Although we did not find inhibition by Arbidol of the H5 coated S-FLU, we have since confirmed inhibition of S-FLU coated with H7 haemagglutinins from A/Netherlands/219/2003 and A/Shanghai/1/2013/H7, as well as H1 haemagglutinins from A/PR/8/1934 and A/England/195/2009 (Data not shown). A recent structure revealed Arbidol bound to H7 haemagglutinin from influenza (87); it may be interesting to analyse the binding of Arbidol to EBOV-GP.

In summary, we have developed a new surrogate E-S-FLU for Ebola virus. It mimics the Ebola virus at the level of cell entry and can be a valuable tool for screening antibodies, drug therapeutics as well as studying the fundamental biology of the Ebola virus entry process.

Materials and Methods

Pseudotyped virus design and production

cDNA encoding EBOV-GP from the following species was human codon optimized and synthesized by GeneArt. (*Zaire Makona* wt/GIN/2014/Kissidougou-C15, Genbank: KJ660346.1). Lentiviral vector pHR-SIN (88) was engineered to incorporate the EBOV-GP cDNA. We transduced Madin-Darby canine kidney epithelial cells (MDCK-SIAT1) (20) with lentivirus to express full-length EBOV-GP.

Transduced cells were stained with EBOV-GP specific monoclonal antibody: KZ52 specific to Zaire (34, 35), or 66-4-C12 cross-reactive to all Ebola Species (Rijal unpublished), and with a second layer of FITC-conjugated goat anti-human antibody (Life technologies ref: H10301). Stained cells were bulk sorted with a fluorescence-activated cell sorter (FACS) to achieve maximal expression of EBOV-GP (E-SIAT cell line, shown in Fig. 1). EBOV-GP was detected on >99% of sorted cells and was stable and uniform up to at least to the 9th passage after sorting.

E-S-FLU was generated based on a non-replicating pseudotyped influenza virus (S-FLU) previously described (11, 89). We used the version that expressed enhanced green fluorescent protein (S-eGFP), which has its S-haemagglutinin coding sequence replaced by an eGFP reporter gene. We isolated subclones of the original S-FLU that showed brighter fluorescence, and found a single mutation at T60C in the A/PR/8/34 Haemagglutinin signal sequence (NCBI Reference Sequence: NC_002017.1) that abrogates an out of frame ATG, which had interfered with downstream eGFP expression. All subsequent versions of S-FLU contain this enhancement, which gives a sufficiently bright fluorescence signal from infected cells to read on the CLARIOstar® fluorescence plate reader. Seed viruses were doubly cloned by limiting dilution before seeding the E-SIAT or H5-SIAT producer cells.

Seed S-FLU viruses coated in H5, H7 or H1 haemagglutinin were titrated by standard TCID50 assay on MDCK-SIAT1 cells, using fluorescence detection (as described below). Titration experiments revealed that a relatively high MOI of approximately 1 TCID50 per cell of seed S-FLU virus (11) added to infect E-SIAT cells produced the highest titers of E-S-FLU, whereas lower MOI (~0.01) was adequate for seeding HA-SIAT cell lines (11). Viral growth medium (VGM) was DMEM with 0.1% Bovine Albumin, 10 mM HEPES, 2 mM glutamine, 100 U/ml penicillin and 100 µg/ml streptomycin). After 2 hours incubation of E-SIAT with seed S-FLU, any remaining seed virus was removed by a wash with PBS. Cells were then incubated in VGM medium for 48 hours at 37 ^{o}C, 5% CO_2 incubator without added trypsin. Culture supernatant was harvested and stored into aliquots at -80 ^{o}C. Replication of HA pseudotyped viruses required addition of trypsin as described (11).

Seed Virus TCID50

Seed S-FLU viruses coated in influenza hemagglutinin were titrated for the concentration of replication competent clones (TCID50) by a standard limiting dilution method as described (Powell et al). Wells containing clones of eGFP expressing S-FLU > 4 Standard Deviations above 16 control wells were detected by plate reader (described below), and the TCID50/ml calculated by the Reed Muench method (90).

S-FLU Batch Cell Infectious Dose 50 (CID50)

Batches of E-S-FLU and H5-S-FLU were titrated for infectivity of MDCK-SIAT1 indicator cells after overnight infection. Harvested culture supernatants (100 ul) containing E-S-FLU or H5 S-FLU were titrated in two-fold dilutions in VGM across a flat-bottomed 96-well plate (Fig. 2A). MDCK-SIAT1 indicator cells were washed in PBS, and $3x10^4$ cells in 100ul VGM were added to each well and incubated for 18 hours (37 ^{o}C, 5% CO_2). Medium was removed from the wells and cells were fixed in 10% formalin (in PBS) for 30 minutes at 4 ^{o}C. The virus titer was assessed by eGFP fluorescence analyzed by plate reader (CLARIOstar®). The dilution of virus in giving 50% of the maximum plateau fluorescence signal (EC50) was calculated by linear interpolation. The EC50 dilution obtained by best fit of the titration curve to the Poisson Distribution was very similar (data not shown). Typical EC50 dilutions for E-S-FLU harvested after 48 hours were ~1:8 compared to ~1: 500 for H5-S-FLU (Fig. 2). From the EC50 dilution, and the number of cells per well ($3x10^4$), the Cell Infectious Dose 50% (CID50/ml) in the E-S-FLU batch was calculated as ~$2X10^6$ CID50/ml, H5 S-FLU as ~$1.6x10^8$ CID50/ml. H5-S-FLU and E-S-FLU were used at a concentration for inhibition assays that gave close to maximum plateau fluorescence in infected MDCK-SIAT1 cells (MOI ~ 4 CID50/cell).

This value of was used to normalise fluorescence readout to % of maximum in the figures (Fig. 2A).

In this paper, all the evaluation and screening were done on Zaire (C15) E-S-FLU and H5-S-FLU in parallel.

CLARIOstar® plate reader setting

Fluorescence plate readout was carried out in costar-96-well cell culture plates (costar #3799). We chose the "COSTAR 96 microplate" mode in the CLARIOstar® software. For measuring eGFP level, fluorescence excitation was at 483nm (bandwidth of 8nm) and emission at 515nm (bandwidth 8nm), with dichroic filter of 499nm. Each well had 50 flashes at 4mm diameter and fluorescence readout from the top optic, giving the orbital averaging value. For measuring WGA (Alexa Fluor® 647 Conjugate) in the drug inhibition assay, fluorescence excitation was at 630nm (bandwidth of 30nm), emission at 678nm (bandwidth of 20nm). Each well had 53 flashes at 4mm and fluorescence readout from the top optic, giving the orbital averaging value. The focal length and gain were adjusted before each plate was read. Generally optimal focal length was 5.0 mm, and gain for eGFP channel was adjusted to 3000; gain for WGA-647 was adjusted to 2500.

E-S-FLU infection in NPC1 knockout cells

Niemann Pick C1 protein (NPC1) is the key receptor for Ebola virus cell entry at the level of the lysosomal membrane (30-32). Two NPC1-knockout HeLa cell lines were generated by the CRISPR/cas9 technique (ex2 NPC1-KO and ex4 NPC1-KO, named by the exon which was deleted). Generation and verification of the NPC1 KO cell lines have been described in Tharkeshwar et al., 2017 (33).

$1X10^5$ wild-type HeLa, ex2 NPC1-KO or ex4 NPC1-KO HeLa cells were seeded to a 24-well tissue culture plate in 500 µl D10 medium (DMEM + 10% foetal calf serum + penicillin and streptomycin) the night before infection. Before infection, the medium was removed and cells were washed once with PBS. Cells were infected with maximal doses of 1 x 10^6 CID50 E-S-FLU (MOI ~10) or 8 x 10^7 CID50 H5-S-FLU (MOI ~800) incubated overnight. After infection, cells were trypsinised and transferred to 5ml polypropylene tubes. Percentage infection was analyzed by counting fluorescent cells in the flow cytometer (CyAn ADP Analyzer).

Micro-neutralization assay

Micro-neutralization assay measures the inhibition titer of antibodies against virus entry *in vitro*. Assay was done as described in Powell et al., 2012 (11, 91) with minor modifications. E-S-FLU (MOI ~4) and H5-S-FLU (MOI ~4) viruses were diluted in VGM to give plateau expression of eGFP in $3X10^4$ MDCK-SIAT1 cells after overnight infection in 96-well flat-bottomed plates. 50 µl of virus was pre-incubated with 50 µl antibody at two-fold dilutions for 2 hours. $3X10^4$ MDCK-SIAT1 cells in 100µl VGM were then seeded to each well and allow overnight infection (37 ^oC, 5% CO2). After infection, medium was removed from the wells and cells were fixed with 100 µl 10% formalin (in PBS) for 30 minutes at 4 ^oC, the formalin then replaced with 100 µl PBS. Plates were analyzed by fluorescence plate reader (CLARIOstar®) and fluorescence microscopy. The concentration of antibody or drug that gave 50% inhibition of infection (IC50%) was calculated by linear interpolation. Monoclonal antibodies mentioned in this study: KZ52, a human monoclonal antibody that specifically binds Zaire EBOV-GP and neutralizes EBOV wild-type virus *in vitro* (34, 35, 92). Our version was reconstituted from the sequence published in the crystal structure PDB file: 3CSY (35). 21D85A is a human monoclonal antibody made in-house that specifically binds to H5 haemagglutinin and neutralizes H5-S-FLU.

We were kindly provided with some EBOV-GP pseudotyped lentivirus (GP-lenti) from Dr. Edward Wright. GP-lenti carries a firefly luciferase reporter gene. 50 μl of GP-lenti pseudotyped viruses were pre-incubated with 50 μl antibodies in two-fold dilutions for 2 hours and $3X10^4$ MDCK-SIAT1 cells were added. Cells were incubated with virus infection in VGM for 48 hours. After 48 hours, infection was quantified by measuring the luciferase reporter expression. Medium was removed from the wells, and cells were lysed with 50 μl Glo-lysis buffer for 5 minute, then 50 μl Bright-Glo (Promega) substrate was added for 5 minute enzymatic reaction. Solutions were transferred to Opaque plates for luminescence measurement using the GloMax®-Multi Detection System (Promega).

Drug inhibition assay

All small inhibitor molecules, including the LOPAC®1280 library mentioned in this study were ordered from Sigma-Aldrich, and stored in 10mM DMSO at -20°C, with the exception of AY9944, which was ordered from Merck (Cat. No. 190080); and trans-Ned19 (provided by our collaborator Antony Galione). Drugs were diluted in VGM to give a starting concentration of 100μM (unless stated otherwise), and then titrated in

50µl VGM in two-fold dilutions across a 96-well plate. $3X10^4$ MDCK-SIAT1 cells were seeded in 50 µl VGM to pre-incubate with drugs for 3 hours (37°C, 5% CO2). 100µl of E-S-FLU (MOI ~4) or H5-S-FLU (MOI ~4) viruses were diluted in VGM to give plateau expression of eGFP in $3X10^4$ MDCK-SIAT1 cells was then added for overnight infection. Cells were fixed with 100 µl 10% formalin (in PBS) for 30 minutes, the formalin was then replaced by PBS, and the plates were analyzed by fluorescence plate reader (CLARIOstar®) as for the MN assay. Infection and inhibition was quantified by measuring the eGFP expression level. IC50 of drug is the concentration at which the eGFP fluorescence signal was reduced by 50%. When more than three measurements were made for each drug, a 95% confidence interval was calculated and stated (Table 1).

Due to the toxicity effect of many drug molecules to cells at high concentrations, dead cells were washed away before plate reading. This may give a falsely low eGFP fluorescence reading in the plate reader, but can be detected by visual inspection in the fluorescence microscope. To estimate the number of cells remaining in each well, plates were stained with wheat germ agglutinin (WGA) after cells were fixed and washed once with phosphate-buffered saline (PBS). WGA is a lectin that binds to sialic acid and N-acetylglucosaminyl residues at the cell surface. 50 µl of 5 µg/ml WGA (Alexa Fluor® 647 Conjugate, Thermofisher Cat: W32466) was added to each well and incubated at room temperature for 15 minutes. Plates were then washed twice with PBS before reading (See the plate reader setting in earlier section.).

LOPAC®1280 screen vs. Johansen et al., drug screen

Johansen et al., (38) screened 2635 compounds for antiviral activity against genetically engineered Ebola virus that expresses eGFP (eGFP-EBOV) *in vitro*. In their supplementary table S1, they have listed all the experimental data for the small molecules they have screened in the study. Out of the 2635 molecules they tested, 538 molecules were also found within the sigma LOPAC®1280 library, and were screened against E-S-FLU in our study. We have compared the inhibitory effect of these 538 compounds in both screens, i.e. each molecule is either "+" (inhibited infection) or "-" (did not inhibit infection within the concentration range tested) and carried out a Fisher's exact test to measure the significance of the association.

LogP and pKa calculation

For the drug molecules listed in Table 1, logP (partition parameter) and pKa values (strongest basic pKa) were estimated by using MarvinSketch program, based on their chemical structure.

Acknowledgements

We thank the MRC of Great Britain, Clarendon Fund, Exeter College Mandarin Scholarship and Radcliffe Department of Medicine for funding, Rod Daniels for sequencing S-FLU clones with bright eGFP fluorescence, Arthur Huang for the antibody 21D85A. We also thank Nick Platt, Fran Platt, Antony Galione and Derek Terrar for their helpful comments on the manuscript.

Reference:

1. Martines RB, Ng DL, Greer PW, Rollin PE, Zaki SR. 2015. Tissue and cellular tropism, pathology and pathogenesis of Ebola and Marburg Viruses. J Pathol 235:153–174.
2. Leroy EM, Kumulungui B, Pourrut X, Rouquet P, Hassanin A, Yaba P, Délicat A, Paweska JT, Gonzalez J-P, Swanepoel R. 2005. Fruit bats as reservoirs of Ebola virus. Nature 438:575–576.
3. Emond RT, Evans B, Bowen ET, Lloyd G. 1977. A case of Ebola virus infection. Br Med J 2:541–4.
4. Burke J, Declerq R, Ghysebrechts G. 1978. Ebola haemorrhagic fever in Zaire, 1976. Report of an international commission. Bull World Health Organ 56:271–293.
5. Kuhn JH, Becker S, Ebihara H, Geisbert TW, Johnson KM, Kawaoka Y, Lipkin WI, Negredo AI, Netesov SV., Nichol ST, Palacios G, Peters CJ, Tenorio A, Volchkov VE, Jahrling PB. 2010. Proposal for a revised taxonomy of the family Filoviridae: classification, names of taxa and viruses, and virus abbreviations. Arch Virol 155:2083–2103.
6. Henao-Restrepo AM, Longini IM, Egger M, Dean NE, Edmunds WJ, Camacho A, Carroll MW, Doumbia M, Draguez B, Duraffour S, Enwere G, Grais R, Gunther S, Hossmann S, Kondé MK, Kone S, Kuisma E, Levine MM, Mandal S, Norheim G, Riveros X, Soumah A, Trelle S, Vicari AS, Watson CH, Kéïta S, Kieny MP, Røttingen J-A. 2015. Efficacy and effectiveness of an rVSV-vectored vaccine expressing Ebola surface glycoprotein: interim results from the Guinea ring vaccination cluster-randomised trial. Lancet 386:857–866.

7. Lee JE, Saphire EO. 2009. *Ebolavirus* glycoprotein structure and mechanism of entry. Future Virol 4(6):621-635

8. Wool-Lewis RJ, Bates P. 1998. Characterization of Ebola virus entry by using pseudotyped viruses: identification of receptor-deficient cell lines. J Virol 72:3155–3160.

9. Takada A, Robison C, Goto H, Sanchez A, Murti KG, Whitt MA, Kawaoka Y. 1997. A system for functional analysis of Ebola virus glycoprotein. Proc Natl Acad Sci U S A 94:14764–14769.

10. Wilkinson DE, Page M, Mattiuzzo G, Hassall M, Dougall T, Rigsby P, Stone L, Minor P. 2017. Comparison of platform technologies for assaying antibody to Ebola virus. Vaccine 35:1347–1352.

11. Powell TJ, Silk JD, Sharps J, Fodor E, Townsend ARM. 2012. Pseudotyped Influenza A Virus as a Vaccine for the induction of Heterotypic Immunity. J Virol 86:13397–13406.

12. Francica JR, Matukonis MK, Bates P. 2009. Requirements for cell rounding and surface protein down-regulation by Ebola virus glycoprotein. Virology 383:237–247.

13. Mohamadzadeh M, Chen L, Schmaljohn AL. 2007. How Ebola and Marburg viruses battle the immune system. Nat Rev Immunol 7:556–567.

14. Simmons G, Wool-lewis RJ, Netter RC, Bates P, Baribaud F. 2002. Ebola Virus Glycoproteins Induce Global Surface Protein Down-Modulation and Loss of Cell Adherence Ebola Virus Glycoproteins Induce Global Surface Protein Down-Modulation and Loss of Cell Adherence. J Virol 76:2518–2528.

15. Takada A, Watanabe S, Ito H, Okazaki K, Kida H, Kawaoka Y. 2000.

Downregulation of beta1 integrins by Ebola virus glycoprotein: implication for virus entry. Virology 278:20–26.

16. Volchkov VE, Volchkova VA, Mühlberger E, Kolesnikova LV, Weik M, Dolniko, Klenk H. 2001. Recovery of Infectious Ebola Virus from Complementary DNA: RNA Editing of the GP Gene and Viral Cytotoxicity. Science (80-) 291:1965–1969.

17. Mohan GS, Ye L, Li W, Monteiro A, Lin X, Sapkota B, Pollack BP, Compans RW, Yang C. 2015. Less Is More: Ebola Virus Surface Glycoprotein Expression Levels Regulate Virus Production and InfectivityJournal of Virology.

18. Alazard-Dany N, Volchkova V, Reynard O, Carbonnelle C, Dolnik O, Ottmann M, Khromykh A, Volchkov VE. 2006. Ebola virus glycoprotein GP is not cytotoxic when expressed constitutively at a moderate level. J Gen Virol 87:1247–1257.

19. Yang ZY, Duckers HJ, Sullivan NJ, Sanchez A, Nabel EG, Nabel GJ. 2000. Identification of the Ebola virus glycoprotein as the main viral determinant of vascular cell cytotoxicity and injury. Nat Med 6:886–889.

20. Matrosovich M, Matrosovich T, Carr J, Roberts NA, Klenk H-D. 2003. Overexpression of the alpha-2,6-Sialyltransferase in MDCK Cells Increases Influenza Virus Sensitivity to Neuraminidase Inhibitors. J Virol 77:8418–8425.

21. Baz M, Boonnak K, Paskel M, Santos C, Powell T, Townsend A. 2015. Nonreplicating Influenza A Virus Vaccines Confer Broad Protection against Lethal Challenge 6:1–13.

22. Chen BJ, Leser GP, Morita E, Lamb R a. 2007. Influenza virus hemagglutinin and neuraminidase, but not the matrix protein, are required for assembly and budding of plasmid-derived virus-like particles. J Virol 81:7111–7123.

23. Jin H, Leser GP, Lamb RA. 1994. The influenza virus hemagglutinin cytoplasmic tail is not essential for virus assembly or infectivity. EMBO J 13:5504–15.

24. Jin H, Leser GP, Zhang J, Lamb RA. 1997. Influenza virus hemagglutinin and neuraminidase cytoplasmic tails control particle shape. EMBO J 16:1236–1247.

25. Melikyan GB, Lin S, Roth MG, Cohen FS. 1999. Amino acid sequence requirements of the transmembrane and cytoplasmic domains of influenza virus hemagglutinin for viable membrane fusion. Mol Biol Cell 10:1821–1836.

26. Rossman J, Lamb R. 2011. Influenza virus assembly and budding. Virology 411:229–236.

27. Schroth-Diez B, Ponimaskin E, Reverey H, Schmidt MF, Herrmann A. 1998. Fusion activity of transmembrane and cytoplasmic domain chimeras of the influenza virus glycoprotein hemagglutinin. J Virol 72:133–41.

28. Zhang J, Pekosz A, Lamb RA. 2000. Influenza virus assembly and lipid raft microdomains: a role for the cytoplasmic tails of the spike glycoproteins. J Virol 74:4634–44.

29. Zhang J, Leser GP, Pekosz A, Lamb RA. 2000. The Cytoplasmic Tails of the Influenza Virus Spike Glycoproteins Are Required for Normal Genome Packaging. Virology 269:325–334.

30. Côté M, Misasi J, Ren T, Bruchez A, Lee K, Filone CM, Hensley L, Li Q, Ory D, Chandran K, Cunningham J. 2011. Small molecule inhibitors reveal Niemann-Pick C1 is essential for Ebola virus infection. Nature 477:344–348.

31. Carette JE, Raaben M, Wong AC, Herbert AS, Obernosterer G, Mulherkar N, Kuehne AI, Kranzusch PJ, Griffin AM, Ruthel G, Dal Cin P, Dye JM, Whelan SP, Chandran K, Brummelkamp TR. 2011. Ebola virus entry requires the cholesterol

transporter Niemann-Pick C1. Nature 477:340–343.

32. Miller EH, Obernosterer G, Raaben M, Herbert AS, Deffieu MS, Krishnan A, Ndungo E, Sandesara RG, Carette JE, Kuehne AI, Ruthel G, Pfeffer SR, Dye JM, Whelan SP, Brummelkamp TR, Chandran K. 2012. Ebola virus entry requires the host-programmed recognition of an intracellular receptor. EMBO J 31:1947–1960.

33. Tharkeshwar AK, Trekker J, Vermeire W, Pauwels J, Sannerud R, Priestman DA, te Vruchte D, Vints K, Baatsen P, Decuypere J-P, Lu H, Martin S, Vangheluwe P, Swinnen J V., Lagae L, Impens F, Platt FM, Gevaert K, Annaert W. 2017. A novel approach to analyze lysosomal dysfunctions through subcellular proteomics and lipidomics: the case of NPC1 deficiency. Sci Rep 7:41408.

34. Maruyama T, Rodriguez LL, Jahrling PB, Sanchez A, Khan AS, Nichol ST, Peters CJ, Parren PWHI, Burton DR. 1999. Ebola Virus Can Be Effectively Neutralized by Antibody Produced in Natural Human Infection. J Virol 73:6024–6030.

35. Lee JE, Fusco ML, Hessell AJ, Oswald WB, Burton DR, Saphire EO. 2008. Structure of the Ebola virus glycoprotein bound to an antibody from a human survivor. Nature 454:177–182.

36. Gehring G, Rohrmann K, Atenchong N, Mittler E, Becker S, Dahlmann F, Pöhlmann S, Vondran FWR, David S, Manns MP, Ciesek S, von Hahn T. 2014. The clinically approved drugs amiodarone, dronedarone and verapamil inhibit filovirus cell entry. J Antimicrob Chemother 69:2123–2131.

37. Sakurai Y, Kolokoltsov AA, Chen C-CC, Tidwell MW, Bauta WE, Klugbauer N, Grimm C, Wahl-schott C, Biel M, Davey RA. 2015. Two-pore channels control Ebola virus host cell entry and are drug targets for disease treatment. Science 347:995–998.

38. Johansen LM, Brannan JM, Delos SE, Shoemaker CJ, Stossel A, Lear C, Hoffstrom BG, Dewald LE, Schornberg KL, Scully C, Lehár J, Hensley LE, White JM, Olinger GG. 2013. FDA-approved selective estrogen receptor modulators inhibit Ebola virus infection. Sci Transl Med 5(190):190ra79.

39. Johansen LM, Dewald LE, Shoemaker CJ, Hoffstrom BG, Lear-rooney CM, Stossel A, Nelson E, Delos SE, Simmons JA, Grenier JM, Pierce LT, Pajouhesh H, Lehár J, Hensley LE, Glass PJ, White JM, Olinger GG. 2015. A screen of approved drugs and molecular probes identifies therapeutics with anti – Ebola virus activity. Sci Transl Med 7:1–14.

40. Saeed MF, Kolokoltsov AA, Albrecht T, Davey RA. 2010. Cellular Entry of Ebola Virus Involves Uptake by a Macropinocytosis-Like Mechanism and Subsequent Trafficking through Early and Late Endosomes. PLoS Pathog 6:e1001110.

41. Kouznetsova J, Sun W, Martínez-Romero C, Tawa G, Shinn P, Chen CZ, Schimmer A, Sanderson P, McKew JC, Zheng W, García-Sastre A. 2014. Identification of 53 compounds that block Ebola virus-like particle entry via a repurposing screen of approved drugs. Emerg Microbes Infect 3:e84.

42. Gnirß K, Kühl A, Karsten C, Glowacka I, Bertram S, Kaup F, Hofmann H, Pöhlmann S. 2012. Cathepsins B and L activate Ebola but not Marburg virus glycoproteins for efficient entry into cell lines and macrophages independent of TMPRSS2 expression. Virology 424:3–10.

43. Basu A, Li B, Mills DM, Panchal RG, Cardinale SC, Butler MM, Peet NP, Majgier-Baranowska H, Williams JD, Patel I, Moir DT, Bavari S, Ray R, Farzan MR, Rong L, Bowlin TL. 2011. Identification of a small-molecule entry inhibitor for filoviruses. J Virol 85:3106–3119.

44. Shoemaker CJ, Schornberg KL, Delos SE, Scully C, Pajouhesh H, Olinger GG, Johansen LM, White JM. 2013. Multiple Cationic Amphiphiles Induce a Niemann-Pick C Phenotype and Inhibit Ebola Virus Entry and Infection. PLoS One 8(2):e56265.

45. Nanbo A, Imai M, Watanabe S, Noda T, Takahashi K, Neumann G, Halfmann P, Kawaoka Y. 2010. Ebolavirus Is Internalized into Host Cells via Macropinocytosis in a Viral Glycoprotein-Dependent Manner. PLoS Pathog 6:e1001121.

46. Shah P, Wang T, Kaletsky R. 2010. A small-molecule oxocarbazate inhibitor of human cathepsin L blocks severe acute respiratory syndrome and ebola pseudotype virus infection into human embryonic. Mol Pharmacol 78:319–324.

47. Chandran K, Sullivan NJ, Felbor U, Whelan SP, Cunningham JM. 2005. Endosomal proteolysis of the Ebola virus glycoprotein is necessary for infection. Science 308:1643–1645.

48. Schornberg K, Matsuyama S, Kabsch K, Delos S, Bouton A, White J. 2006. Role of Endosomal Cathepsins in Entry Mediated by the Ebola Virus Glycoprotein Role of Endosomal Cathepsins in Entry Mediated by the Ebola Virus Glycoprotein. J Virol 80:4174–4178.

49. Linden WA Van Der, Schulze CJ, Herbert AS, Krause TB, Wirchnianski AA, Dye JM, Chandran K, Bogyo M, States U, Detrick F, States U, States U. 2016. Cysteine Cathepsin Inhibitors as Anti-Ebola Agents 2:173–179.

50. Nogales A, Baker SF, Domm W, Mart??nez-Sobrido L. 2016. Development and applications of single-cycle infectious influenza A virus (sciIAV). Virus Res 216:26–40.

51. Hoenen T, Groseth A, Callison J, Takada A, Feldmann H. 2013. A novel Ebola

virus expressing luciferase allows for rapid and quantitative testing of antivirals. Antiviral Res 99:207–213.

52. Li D, Chen T, Hu Y, Zhou Y, Liu Q, Zhou D, Jin X, Huang Z. 2016. An Ebola virus-like particle-based reporter system enables evaluation of antiviral drugs in vivo under non-BSL-4 conditions. J Virol 90:JVI.01239-16.

53. Fan H, Du X, Zhang J, Zheng H, Lu X, Wu Q, Li H, Wang H, Shi Y, Gao G, Zhou Z, Tan D-X, Li X. 2017. Selective inhibition of Ebola entry with selective estrogen receptor modulators by disrupting the endolysosomal calcium. Sci Rep 7:41226.

54. Suárez T, Gómara MJ, Félix M Goñia, Ismael Mingarrob, Arturo Mugaa, Enrique Pérez-Payáb JLN. 2003. Calcium-dependent conformational changes of membrane-bound Ebola fusion peptide drive vesicle fusion. FEBS Lett 535:23–28.

55. Simmons JA, D'Souza RS, Ruas M, Galione A, Casanova JE, White JM. 2016. Ebolavirus Glycoprotein Directs Fusion through NPC1 $^{+}$ Endolysosomes. J Virol 90:605–610.

56. De Duve C, De Barsy T, Poole B, Trouet A, Tulkens P, Van Hoof F. 1974. Lysosomotropic agents. Biochem Pharmacol 23:2495-2531.

57. Kornhuber J, Henkel AW, Groemer TW, Städtler S, Welzel O, Tripal P, Rotter A, Bleich S, Trapp S. 2010. Lipophilic cationic drugs increase the permeability of lysosomal membranes in a cell culture system. J Cell Physiol 224:152–164.

58. Funk RS, Krise JP. 2012. Cationic amphiphilic drugs cause a marked expansion of apparent lysosomal volume: Implications for an intracellular distribution-based drug interaction. Mol Pharm 9:1384–1395.

59. Kornhuber J, Tripal P, Reichel M, Terfloth L, Bleich S, Wiltfang J, Gulbins E.

2008. Identification of new functional inhibitors of acid sphingomyelinase using a structure-property-activity relation model. J Med Chem 51:219–237.

60. Kornhuber J, Muehlbacher M, Trapp S, Pechmann S, Friedl A, Reichel M, Mühle C, Terfloth L, Groemer TW, Spitzer GM, Liedl KR, Gulbins E, Tripal P. 2011. Identification of Novel Functional Inhibitors of Acid Sphingomyelinase. PLoS One 6:e23852.

61. Zhao Y, Ren J, Harlos K, Jones DM, Zeltina A, Bowden TA, Padilla-Parra S, Fry EE, Stuart DI. 2016. Toremifene interacts with and destabilizes the Ebola virus glycoprotein. Nature 535:169–172.

62. Ayad RF, Assar MD, Simpson L, Garner JB, Schussler JM. 2010. Causes and management of drug-induced long QT syndrome. Proc (Bayl Univ Med Cent) 23:250–255.

63. Svanström H, Pasternak B, Hviid A, Svanstrom H, Pasternak B, Hviid A. 2014. Use of clarithromycin and roxithromycin and risk of cardiac death: cohort study. Bmj 349:g4930.

64. Foo B, Williamson B, Young JC, Lukacs G, Shrier A. 2016. hERG quality control and the long QT syndrome. J Physiol 594:2469–2481.

65. Dennis a, Wang L, Wan X, Ficker E. 2007. hERG channel trafficking: novel targets in drug-induced long QT syndrome. Biochem Soc Trans 35:1060–1063.

66. Lounkine E, Keiser MJ, Whitebread S, Mikhailov D, Jenkins J, Lavan P, Weber E, Doak AK, Côté S, Shoichet BK, Urban L. 2012. Large Scale Prediction and Testing of Drug Activity on Side- Effect Targets. Nature 486:361–367.

67. Turone F. 2014. Doctors trial amiodarone for Ebola in Sierra Leone. Bmj 349:g7198.

68. Gupta-Wright a., Lavers J, Irvine S. 2015. Concerns about the off-licence use of amiodarone for Ebola. Bmj 350:h272–h272.

69. Sun W, He S, Martínez-Romero C, Kouznetsova J, Tawa G, Xu M, Shinn P, Fisher EG, Long Y, Motabar O, Yang S, Sanderson PE, Williamson PR, García-Sastre A, Qiu X, Zheng W. 2017. Synergistic drug combination effectively blocks Ebola virus infection. Antiviral Res 137:165–172.

70. Nguyen JT, Hoopes JD, Le MH, Smee DF, Patick AK, Faix DJ, Blair PJ, De Jong MD, Prichard MN, Went GT. 2010. Triple combination of amantadine, ribavirin, and oseltamivir is highly active and synergistic against drug resistant influenza virus strains in vitro. PLoS One 5(2):e9332.

71. Oestereich L, Lüdtke A, Wurr S, Rieger T, Muñoz-Fontela C, Günther S. 2014. Successful treatment of advanced Ebola virus infection with T-705 (favipiravir) in a small animal model. Antiviral Res 105:17–21.

72. Furuta Y, Gowen BB, Takahashi K, Shiraki K, Smee DF, Barnard DL. 2013. Favipiravir (T-705), a novel viral RNA polymerase inhibitor. Antiviral Res.

73. Nagata T, Lefor AK, Hasegawa M, Ishii M. 2015. Favipiravir: A New Medication for the Ebola Virus Disease Pandemic. Disaster Med Public Health Prep 9:79–81.

74. De Clercq E. 2014. Ebola virus (EBOV) infection: therapeutic strategies. Biochem Pharmacol 93:1–10.

75. Liu S, Neidhardt EA, Grossman TH, Ocain T, Clardy J. 2000. Structures of human dihydroorotate dehydrogenase in complex with antiproliferative agents. Structure 8:25–33.

76. Hoffmann H-H, Kunz A, Simon VA, Palese P, Shaw ML. 2011. Broad-spectrum antiviral that interferes with de novo pyrimidine biosynthesis. Proc Natl Acad Sci U

S A 108:5777–5782.

77. McLean JE, Neidhardt EA, Grossman TH, Hedstrom L. 2001. Multiple inhibitor analysis of the brequinar and leflunomide binding sites on human dihydroorotate dehydrogenase. Biochemistry 40:2194–2200.

78. Lucas-Hourani M, Dauzonne D, Jorda P, Cousin G, Lupan A, Helynck O, Caignard G, Janvier G, André-Leroux G, Khiar S, Escriou N, Desprès P, Jacob Y, Munier-Lehmann H, Tangy F, Vidalain P-O. 2013. Inhibition of pyrimidine biosynthesis pathway suppresses viral growth through innate immunity. PLoS Pathog 9:e1003678.

79. Eriksson B, Helgstrand E, Johansson NG, Larsson A, Misiorny A, Norén JO, Philipson L, Stenberg K, Stening G, Stridh S, Oberg B. 1977. Inhibition of influenza virus ribonucleic acid polymerase by ribavirin triphosphate. Antimicrob Agents Chemother 11:946–951.

80. Adinolfi LE, Utili R, Tonziello A, Ruggiero G. 2003. Effects of alpha interferon induction plus ribavirin with or without amantadine in the treatment of interferon non-responsive chronic hepatitis C: A randomised trial. Gut 52:701–705.

81. Markosyan RM, Miao C, Zheng YM, Melikyan GB, Liu SL, Cohen FS. 2016. Induction of Cell-Cell Fusion by Ebola Virus Glycoprotein: Low pH Is Not a Trigger. PLoS Pathog 12(1):e1005373.

82. Jurgeit A, McDowell R, Moese S, Meldrum E, Schwendener R, Greber UF. 2012. Niclosamide Is a Proton Carrier and Targets Acidic Endosomes with Broad Antiviral Effects. PLoS Pathog 8(10):e1002976.

83. Rajamuthiah R, Fuchs BB, Conery AL, Kim W, Jayamani E, Kwon B, Ausubel FM, Mylonakis E. 2015. Repurposing salicylanilide anthelmintic drugs to combat drug

resistant Staphylococcus aureus. PLoS One 10:1–19.

84. Leneva I a., Russell RJ, Boriskin YS, Hay AJ. 2009. Characteristics of arbidol-resistant mutants of influenza virus: Implications for the mechanism of anti-influenza action of arbidol. Antiviral Res 81:132–140.

85. Teissier E, Zandomeneghi G, Loquet A, Lavillette D, Lavergne J-P, Montserret R, Cosset F-L, Böckmann A, Meier BH, Penin F, Pécheur E-I. 2011. Mechanism of inhibition of enveloped virus membrane fusion by the antiviral drug arbidol. PLoS One 6:e15874.

86. Pécheur E-I, Borisevich V, Halfmann P, Morrey JD, Smee DF, Prichard M, Mire CE, Kawaoka Y, Geisbert TW, Polyak SJ. 2016. The synthetic antiviral drug arbidol inhibits globally prevalent pathogenic viruses. J Virol 90:3086–3092.

87. Kadam RU, Wilson IA. 2017. Structural basis of influenza virus fusion inhibition by the antiviral drug Arbidol. Proc Natl Acad Sci 114:206–214.

88. Demaison C, Parsley K, Brouns G, Scherr M, Battmer K, Kinnon C, Grez M, Thrasher AJ. 2002. High-level transduction and gene expression in hematopoietic repopulating cells using a human immunodeficiency [correction of imunodeficiency] virus type 1-based lentiviral vector containing an internal spleen focus forming virus promoter. Hum Gene Ther 13:803–813.

89. Martínez-Sobrido L, Cadagan R, Steel J, Basler CF, Palese P, Moran TM, García-Sastre A. 2010. Hemagglutinin-Pseudotyped Green Fluorescent Protein-Expressing Influenza Viruses for the Detection of Influenza Virus Neutralizing Antibodies. J Virol 84:2157–2163.

90. Reed LJ, Muench H. 1938. A simple method of estimating fifty per cent end points. Am J Hyg (Lond.) 27:493-497.

91. Rowe T, Abernathy RA, Hu-Primmer J, Thompson WW, Lu X, Lim W, Fukuda K, Cox NJ, Katz JM. 1999. Detection of antibody to avian influenza A (H5N1) virus in human serum by using a combination of serologic assays. J Clin Microbiol 37:937–943.

92. Parren PWHI, Geisbert TW, Maruyama T, Jahrling PB, Burton DR. 2002. Pre- and Postexposure Prophylaxis of Ebola Virus Infection in an Animal Model by Passive Transfer of a Neutralizing Human Antibody Pre- and Postexposure Prophylaxis of Ebola Virus Infection in an Animal Model by Passive Transfer of a Neutralizing Human An 76:6408–6412.

Figure legend:

FIG 1 Stable expression of EBOV-GP protein on the surface of transduced MDCK-SIAT1 cell line.

FACS plots of **(A)** MDCK-SIAT1 and **(B)** MDCK-SIAT1 cells transduced with full-length GP (E-SIAT). Cells were stained with primary antibody KZ52 (anti-GP antibody) or 21D85A (anti-H5 antibody), followed by a FITC-linked anti-human secondary antibody. E-SIAT cells stably express GP at the cell surface up to at least the 9th passage, which can be detected by a conformational antibody KZ52 specifically (**B**: blue).

(C to F) Immunofluorescence pictures of MDCK-SIAT1 **(C and E)**, E-SIAT **(D and F)** stained with KZ52 and FITC-linked anti-human antibody.

FIG 2 Pseudotyping S-FLU with EBOV-GP.

(A) E-SIAT cells were seeded with 1 TCID50 per cell of seed S-FLU virus to generate EBOV-GP (cyan) and H5 (red) pseudotyped S-FLU viruses. Parental MDCK-SIAT1 cells were also included as control. Culture supernatant (s/n) harvested after 48 hours was titrated in comparison to H5-S-FLU in two-fold dilutions on MDCK-SIAT1 indicator cells for 24 hours infection. Infected cells expressing eGFP were detected and quantified by a CLARIOstar® fluorescence plate reader. Undiluted E-S-FLU and H5-S-FLU gives a saturated infection and the maximum fluorescence readout is used to calculate the infection% at lower dilutions.

(B) E-SIAT and H5-SIAT cells were seeded with 1 TCID50 per cell of seed S-FLU virus. Culture supernatant harvested at different time points post seeding were titrated on MDCK-SIAT1 cells. The EC50 is the dilution of virus giving 50% of the maximum plateau fluorescence signal and was calculated by linear interpolation. The CID50/ml is calculated from the EC50 dilution and the number of cells per well ($3X10^4$ cells).

(C) 100 TCID50 seed S-FLU virus was added to $3X10^4$ MDCK-SIAT1, E-SIAT or H5-SIAT cells. Live images of representative plaques were taken by IncuCyte® every 3 hours. E-SIAT supports formation of small diffuse plaque compared to the dense plaque formed in H5-SIAT cells.

FIG 3 E-S-FLU requires NPC1 receptor expression for infection of HeLa cells. FACS plots of wild-type HeLa cells and two clones of NPC1 knockout HeLa cells (ex2 NPC1-KO and ex4 NPC1-KO) infected by undiluted E-S-FLU and H5-S-FLU. S-FLU encodes an eGFP reporter gene. Percentage infected cells is indicated by percentage of cells with GFP readout higher than 10^2.

FIG 4 Antibody neutralisation of pseudotyped influenza virus E-S-FLU, H5-S-FLU, and lentivirus HIV(EBOV-Z) pseudotype.

Viruses were pre-incubated for 2 hours with antibody KZ52 (anti-GP) or 21D85A (anti-H5) before adding the indicator MDCK-SIAT 1 cells. Antibodies were titrated in two-fold dilutions from 10µg/ml. After 24 hours, infection was quantified by measuring the eGFP expression (influenza) or luminenscence (lentivirus). Titration curves are shown in **(A), (B)** and **(C).** EC50 of an antibody is the concentration at which infection is reduced by 50%. Summary of EC50 concentrations for mAb KZ52 and 21D85A to the three pseudotyped viruses is shown in **(D)**. Multiple EC50 values from repeat experiments are shown with their geometric mean and 95% confident intervals. 10,000 ng/ml is assigned to antibodies that did not neutralize.

(E and F) Microscopy pictures (X10 objective) of assays showing specificity of micro-neutralisation by antibodies. For "Virus only", E-S-FLU and H5-S-FLU were added directly to MDCK-SIAT1 cells. Infected cells express eGFP, shown as green cells. In the MN assay, virus was pre-incubated with 10 µg/ml of monoclonal antibody KZ52 (anti-GP) or 21D85A (anti-H5) before infecting MDCK-SIAT1 cells. Inhibition is visualized as significant reduced green fluorescent cells.

FIG 5 Tetrandrine inhibition assay with E-S-FLU and H5-S-FLU.

Tetrandrine was titrated from 100uM to 0.2uM in the drug inhibition assay against E-S-FLU and H5-S-FLU. Cells were pre-incubated with Tetrandrine for 3 hours and infected by virus for 24 hours. **(A)** Infection% was quantified by eGFP expression measured by fluorescence plate reader. **(B)** WGA was added to stain cell membrane sialic acid and N-acetylglucosaminyl residues, as an estimation of cell number remaining in each well after fixation and wash. Toxicity reduces the WGA fluorescence as cells detach from the plastic. Note that the S-FLU expresses neuraminidase which partially reduces WGA binding in (B). Neutralisation of S-FLU is associated with some increase in WGA binding as neuraminidase expression is reduced.

(C and D) Microscopy pictures of Tetrandrine inhibition assay. Note that toxicity of Tetrandrine at 25uM resulted in reduction in cells in the brightfield channel.

FIG 6 Groups of drugs from the LOPAC1280 library inhibited E-S-FLU. 215 out of 1280 small molecules inhibited E-S-FLU infection. They were grouped and displayed according to their pharmacological activities. Number displayed indicate number of drug molecules inhibited E-S-FLU from this group.

FIG 7 Summary of all the drugs (228 molecules) that have inhibited E-S-FLU in this study. This includes 215 inhibitors from LOPAC1280 library and 13 additional inhibitors tested. 25 molecules inhibited H5-S-FLU, all of which also inhibited E-S-FLU. The inhibitors were ranked and plotted according to their IC50 concentration, at which 50% of the virus infection is inhibited. (Titration example shown in Fig. 5). Detailed information of the inhibitors are listed in supplementary Table S1.

FIG 8 Ebola virus cell entry mechanism (adapted from J White and K Schornberg 2012 Nature Rev. Microbiol) and potential drug mode of actions.

Table 1 IC50 of 13 drugs that inhibited E-S-FLU infection selected from the literature

Table 2 Comparison of overlapping set of drugs between LOPAC1280 library and the collection of Johansen et al., 2015 (39).

538 drug molecules appeared in both our LOPAC1280 library screen and the Johansen et al., 2015's screen. "+" indicates the number of inhibitors, and "–" indicates the non-inhibitors. Association between two screens are calculated by two-tailed Fisher's exact test.

Table 3 25 small molecules that inhibited both E-S-FLU and H5-S-FLU in this study. (22 come from LOPAC1280 library).

Table 1 IC50 of 13 drugs that inhibited E-S-FLU infection selected from the literature

Drug (Rank in Supplementary Table S1)	Mechanism	E-S-FLU IC50 (μM) Geometric mean (95% C.I.)	IC50 in the literature (μM)	Virus	Reference	LogP	pKa (strongest basic)
Amiodarone (No. 18)	Calcium channel inhibitor	2.04 (0.54~7.76)	0.4	Wild-type EBOV	Gehring et al., 2014	7.2	8.5
Verapamil (No. 71)		10.6 (2.75~9.8)	3.1	Wild-type EBOV	Sakurai et al., 2015	3.8	9.7
Tetrandrine (No. 13)		1.63 (0.65~4.07)	0.06	Wild-type EBOV	Sakurai et al., 2015	5.6	8.3
Clomiphene (No. 6)	Estrogen receptor antagonist	0.35 (0.23~0.55)	2.4	Wild-type EBOV	Johansen et al., 2013	6.1	9.3
Toremifene (No. 1)		0.15 (0.14~0.16)	0.2	Wild-type EBOV	Johansen et al., 2013	5.7	8.8
Imipramine (No.33)	Anti-depressant	3.82 (2.51~5.75)	13.7	EBOV (VLPs)	Kouznetsova et al., 2014	4.5	9.4
Clarithromycin (No. 87)	Antibiotics	14.0 (2.19~91.2)	4.5	EBOV (VLPs)	Kouznetsova et al., 2014	3.2	8.4
U18666A (No. 21)	NPC1 phenotype inducer	2.32 (0.19~28.8)	3.0	rVSV-EBOV-GP	Carette et al., 2011	5.5	9.4
Arbidol (No.39)	Fusion inhibitor	5.17 (0.60~43.7)	5.97	Wild-type EBOV	Johansen et al., 2013	5.1	9.9
EIPA (5-(N-Ethyl-N-Isopropyl) Amiloride (No. 106)	Macropinocytosis inhibitor	17.8 (14.1~22.4)	25.0	Wild-type EBOV	Saeed et al., 2010	0.3	2.3
MDL28170 (No. 32)	Calpain inhibitor	3.81 (0.85~17.0)	10.0	GP pseudotyped lentivirus	Gnirß et al., 2012	2.8	-4.3
E64 (No. 201)	Cathepsin inhibitor	77.2 (64.6~93.3))	50.0	GP pseudotyped lentivirus	Gnirß et al., 2012	-1.1	11.3
Niclosamide (No. 14)	Proton Ionophore	1.69 (1.00~2.88)	2.64	Wild-type EBOV	Johansen et al., 2013	4.1	-4.4

Journal of Virology

Table 2 *Comparison of overlapping set of drugs between LOPAC1280 library and the collection of Johansen et al., 2015.*

Two-tailed Fisher's exact test			
	Johansen +	Johansen -	Total
LOPAC +	23	70	93
LOPAC -	26	419	445
Total	49	489	538
P value: < 0.0001			

538 drug molecules appeared in both our LOPAC1280 library screen and the Johansen et al., 2015's screen. "+" indicates the number of inhibitors, and "–" indicates the non-inhibitors. Association between two screens are calculated by two-tailed Fisher's exact test.

Table 3. 25 small molecules that has inhibited both E-S-FLU and H5-S-FLU in this study. (22 come from LOPAC1280 library)

No. in Table S1	LOPAC Plate No.	Sigma Cat. Number	Name	Highest conc tested (μM)	IC50-E (μM)	IC50-H5 (μM)	Effect
5	12-G4	O3125	Ouabain	1.5	0.28	0.3	reduced
7	14-B2	R1402	Raloxifene HCl	50	0.40	33.8	reduced
14	11-G7	N3510	Niclosamide	25	1.69	3.2	reduced
21		U3633	U18666A	100	2.56	49.5	reduced
27	04-B11	C8903	Clemastine fumarate salt	100	3.40	58.4	reduced
35		SML0445	Clemastine	50	4.30	50.0	reduced
42	04-F7	C6628	Chloroquine diphosphate	200	5.44	67.0	reduced
48	03-B7	PZ0171	CP-100356 monohydrochloride	50	6.80	20.0	reduced
54	02-H5	A9809	Amsacrine hydrochloride	25	7.68	6.76	reduced
61	02-E10	A255	A-77636 hydrochloride	25	8.60	15.6	reduced
63	08-E9	H127	Hexahydro-sila-difenidol hydrochloride, p-fluoro analog	100	9.30	65.0	reduced
70	12-E7	L9793	LP44	100	10.40	70.0	reduced
118	02-C7	PZ0178	PHA 767491 hydrochloride	25	21.30	15.7	reduced
2	01-D5	A1784	Aminopterin	100	0.20	0.2	**dimmer**
11	02-C11	SML0113	Brequinar sodium salt hydrate	100	1.30	1.4	**dimmer**
19	04-D3	C3930	Calmidazolium chloride	6.25	2.30	3.9	**dimmer**
20	03-D6	G6423	Gemcitabine hydrohloride	100	2.50	1.9	**dimmer**
60	05-D6	D0670	Dihydroouabain	25	8.30	5.7	**dimmer**
104	13-B10	SML0678	Pyridostatin trifluoroacetate slt	200	17.40	58.8	**dimmer**
135	05-B9	D3768	Dequalinium chloride hydrate	100	27.30	12.1	**dimmer**
145	14-C9	S3378	Spironolactone	100	30.40	33.1	**dimmer**
159		2778-5 (Cambridge Biosciences)	Faviparivir (T705)	500	39.30	67.3	**dimmer**
209	15-H7	T4143	Triamterene	200	85.20	132.3	**dimmer**
222	15-A8	T4182	Tyrphostin AG 1478	200	115.30	141.0	**dimmer**
226	14-C4	R9644	Ribavirin	200	125.20	125.9	**dimmer**

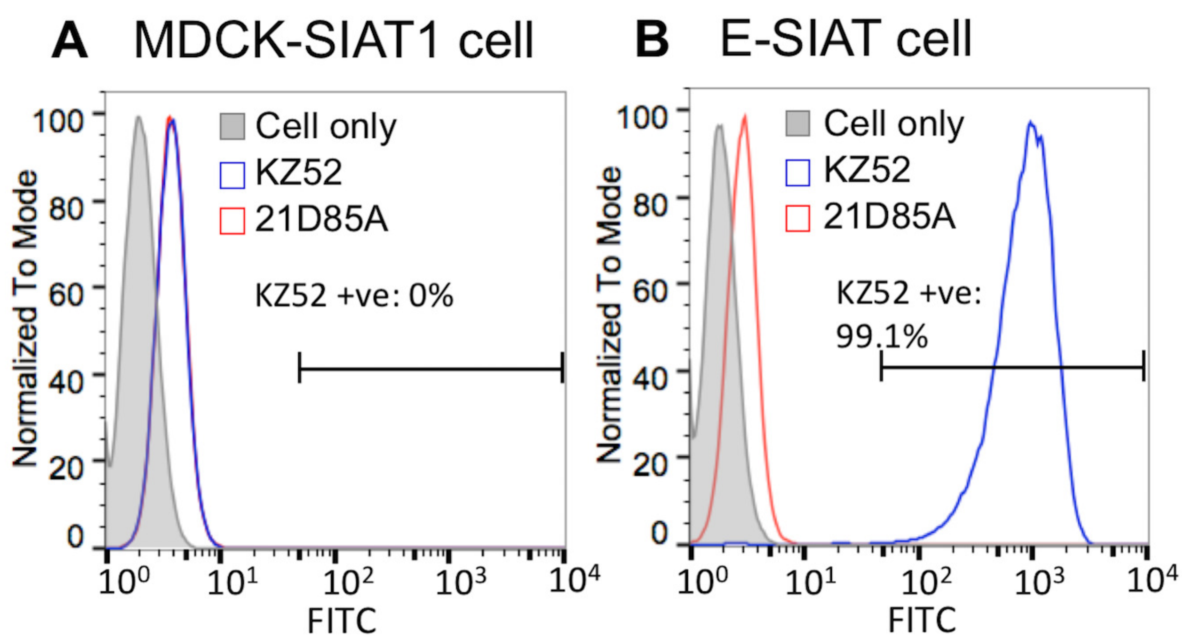
A MDCK-SIAT1 cell
B E-SIAT cell
Cell only
KZ52
21D85A
KZ52 +ve: 0%
KZ52 +ve: 99.1%
Normalized To Mode
FITC
100
80
60
40
20
0
10^0
10^1
10^2
10^3
10^4

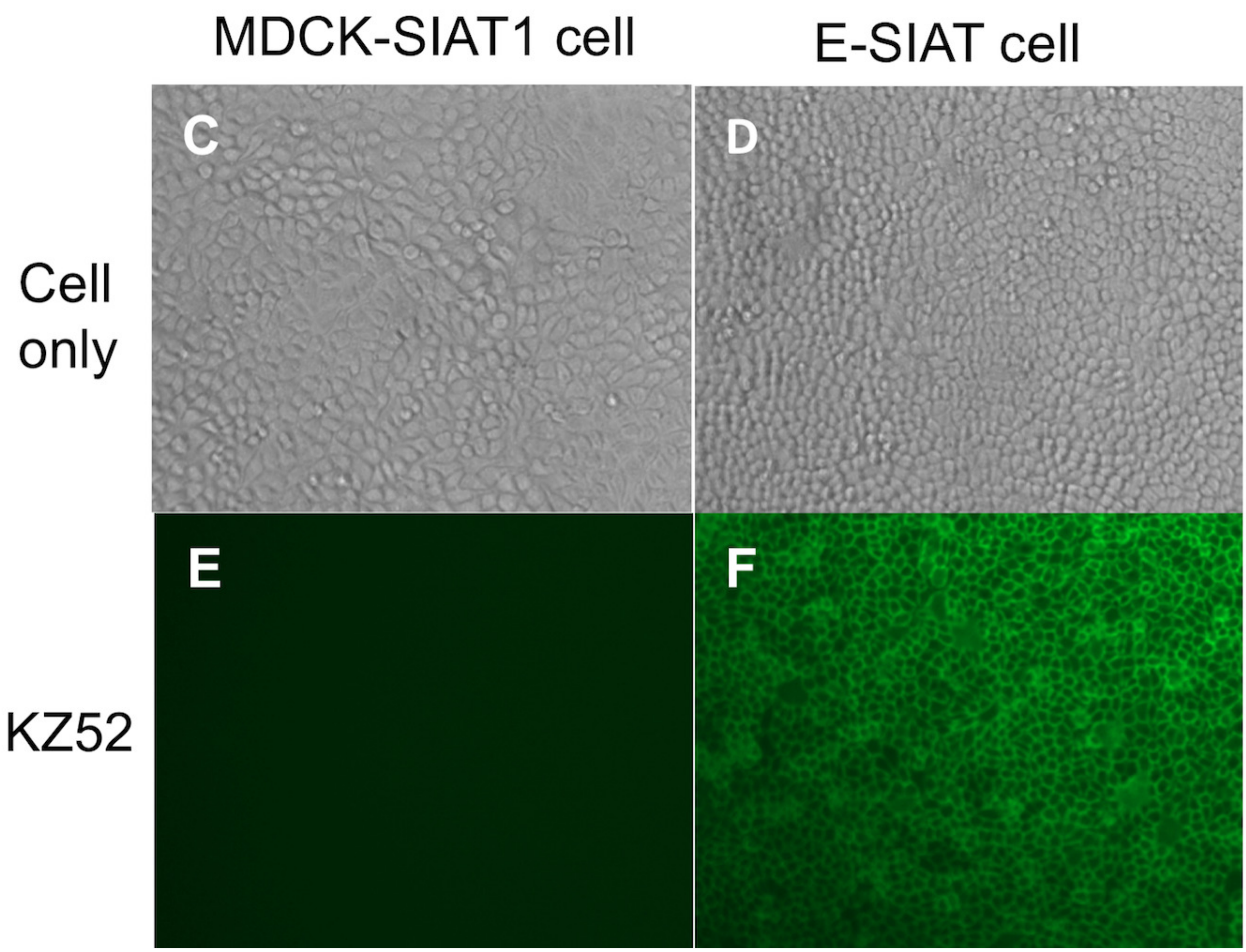
MDCK-SIAT1 cell
E-SIAT cell
C
D
Cell only
E
F
KZ52

A

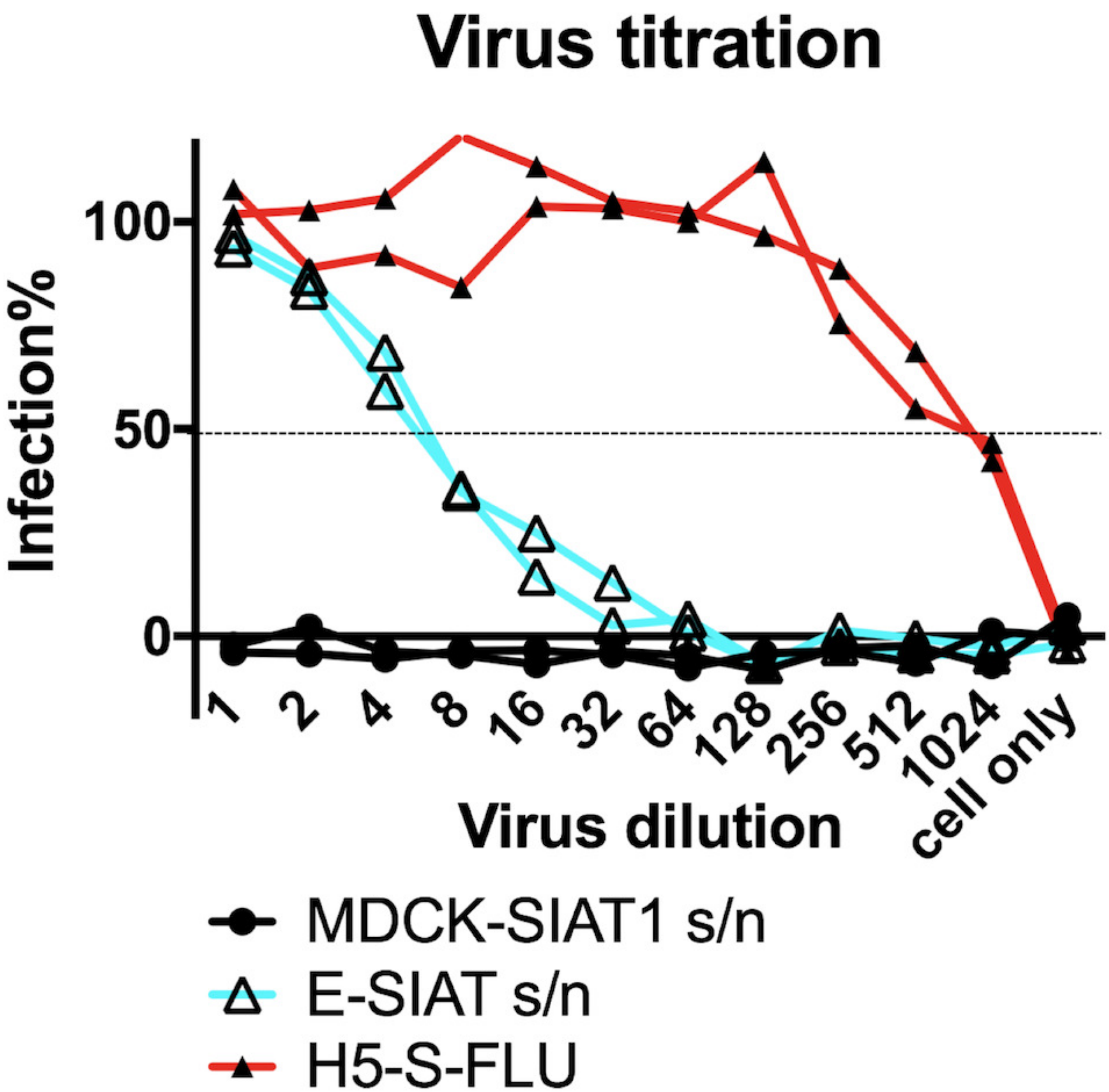
Virus titration
Infection%
100
50
0
1
2
4
8
16
32
64
128
256
512
1024
cell only
Virus dilution
MDCK-SIAT1 s/n
E-SIAT s/n
H5-S-FLU

B

Time point (hr)	E-S-FLU CID50/ml	H5-S-FLU CID50/ml
0	NA	NA
6	NA	NA
12	3.2E+05	6.2E+07
18	5.0E+05	2.1E+08
24	5.0E+05	1.5E+08
30	5.6E+05	1.4E+08
36	5.0E+05	8.1E+07
42	5.2E+05	3.3E+07
48	1.6E+06	8.5E+07
54	1.3E+06	2.9E+07
60	4.5E+05	1.1E+07
66	2.2E+06	7.8E+06
72	3.7E+06	1.5E+07

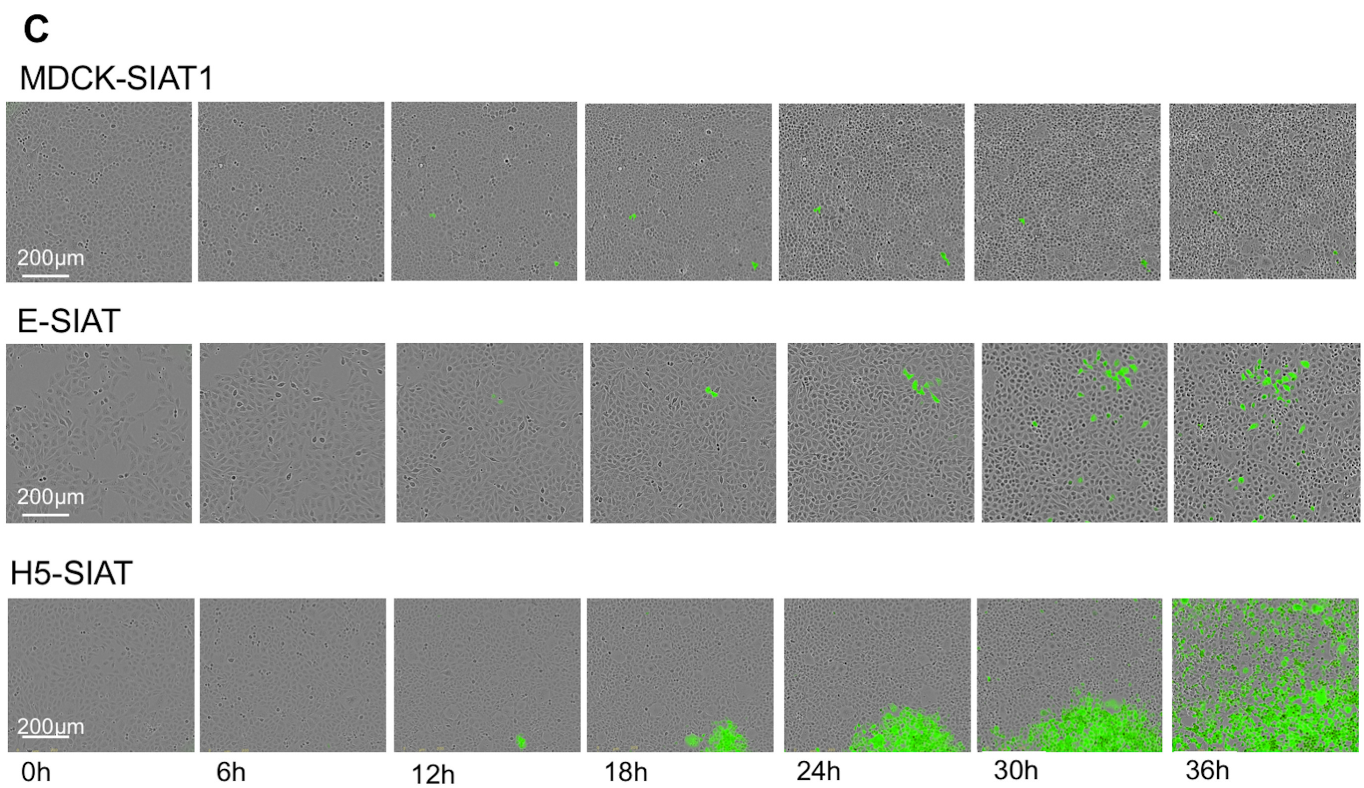
C
MDCK-SIAT1
200μm
E-SIAT
200μm
H5-SIAT
200μm
0h
6h
12h
18h
24h
30h
36h

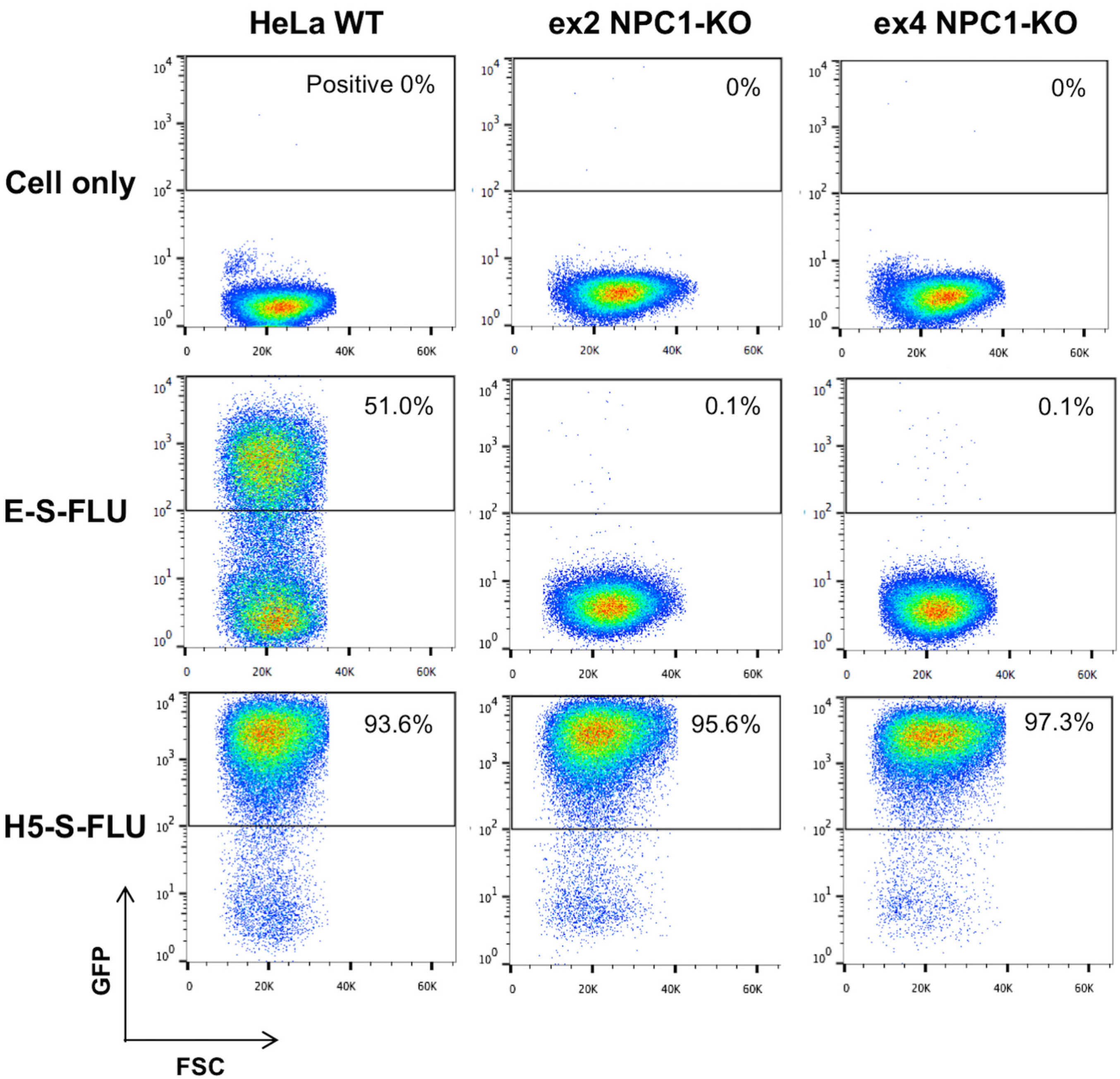
HeLa WT
ex2 NPC1-KO
ex4 NPC1-KO
Cell only
E-S-FLU
H5-S-FLU
Positive 0%
0%
0%
51.0%
0.1%
0.1%
93.6%
95.6%
97.3%
GFP
FSC

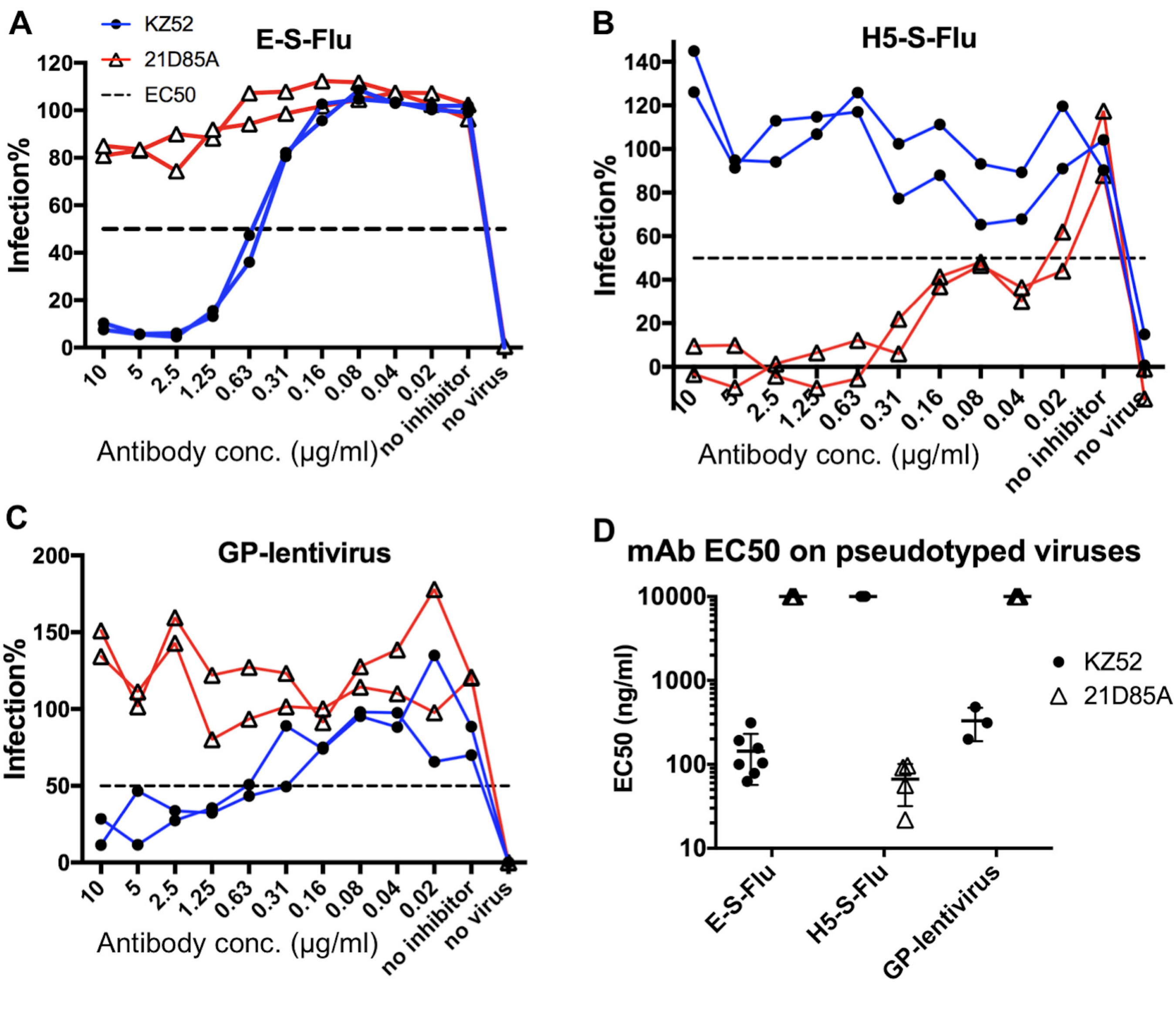
A
E-S-Flu
KZ52
21D85A
EC50
Infection%
120
100
80
60
40
20
0
10
5
2.5
1.25
0.63
0.31
0.16
0.08
0.04
0.02
no inhibitor
no virus
Antibody conc. (µg/ml)
B
H5-S-Flu
Infection%
140
120
100
80
60
40
20
0
Antibody conc. (µg/ml)
C
GP-lentivirus
Infection%
200
150
100
50
0
Antibody conc. (µg/ml)
D
mAb EC50 on pseudotyped viruses
EC50 (ng/ml)
10000
1000
100
10
E-S-Flu
H5-S-Flu
GP-lentivirus
KZ52
21D85A

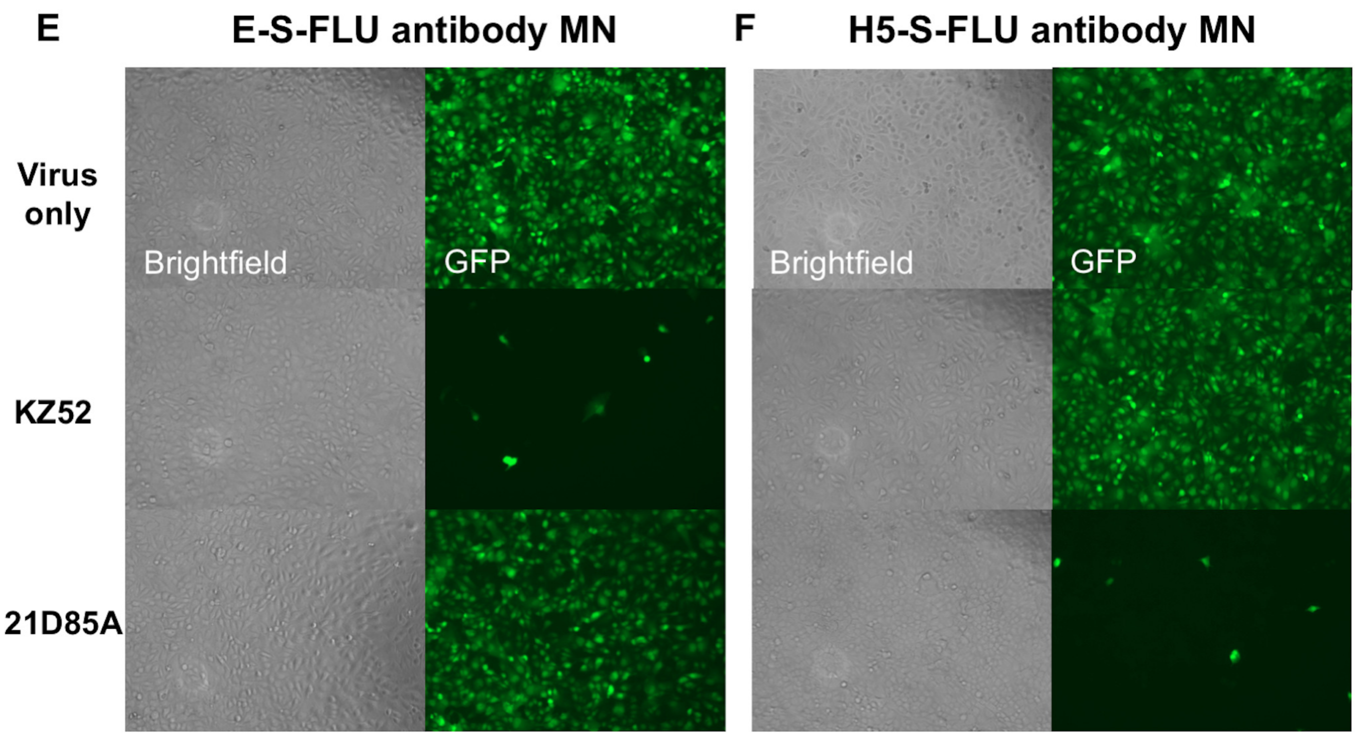

Journal of Virology

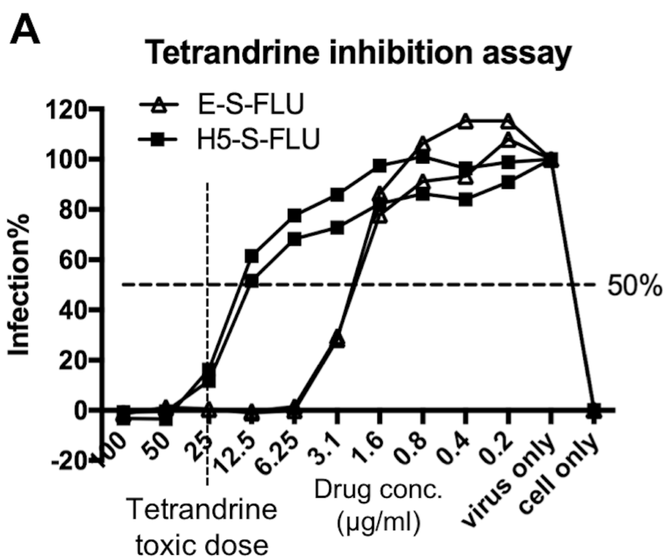
A
Tetrandrine inhibition assay
E-S-FLU
H5-S-FLU
Infection%
120
100
80
60
40
20
0
-20
50%
100
50
25
12.5
6.25
3.1
1.6
0.8
0.4
0.2
virus only
cell only
Tetrandrine
toxic dose
Drug conc.
(µg/ml)

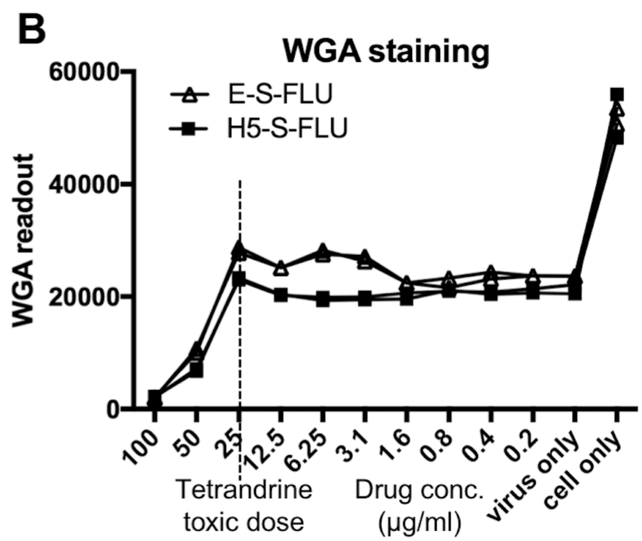
B
WGA staining
E-S-FLU
H5-S-FLU
WGA readout
60000
40000
20000
0
100
50
25
12.5
6.25
3.1
1.6
0.8
0.4
0.2
virus only
cell only
Tetrandrine
toxic dose
Drug conc.
(µg/ml)

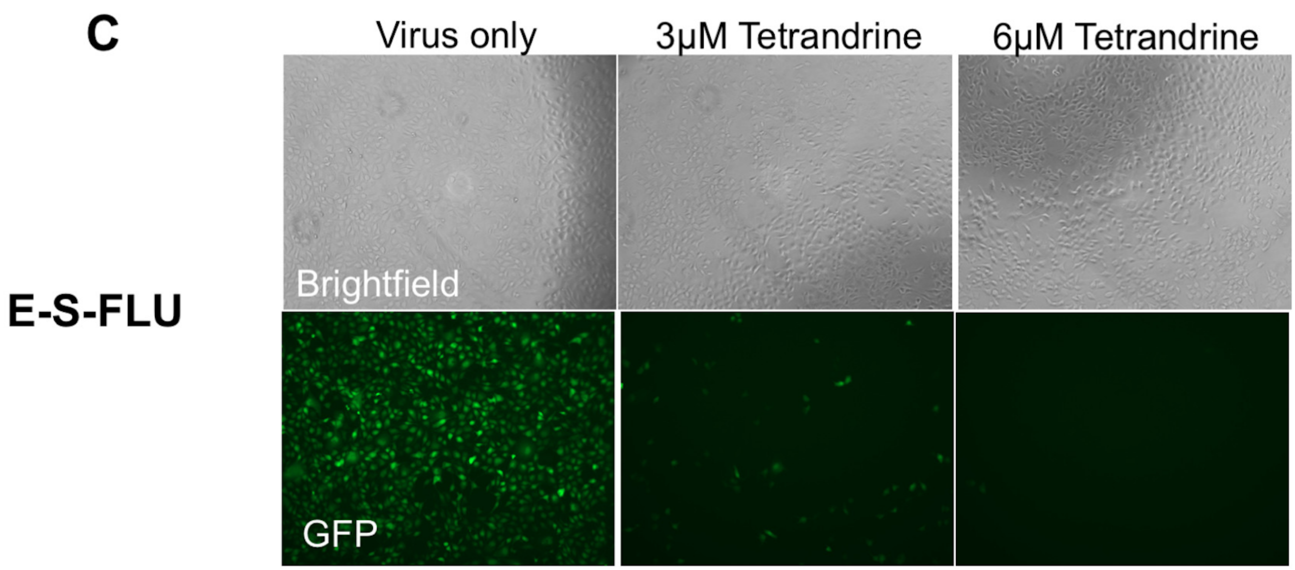
C
Virus only
3μM Tetrandrine
6μM Tetrandrine
E-S-FLU
Brightfield
GFP

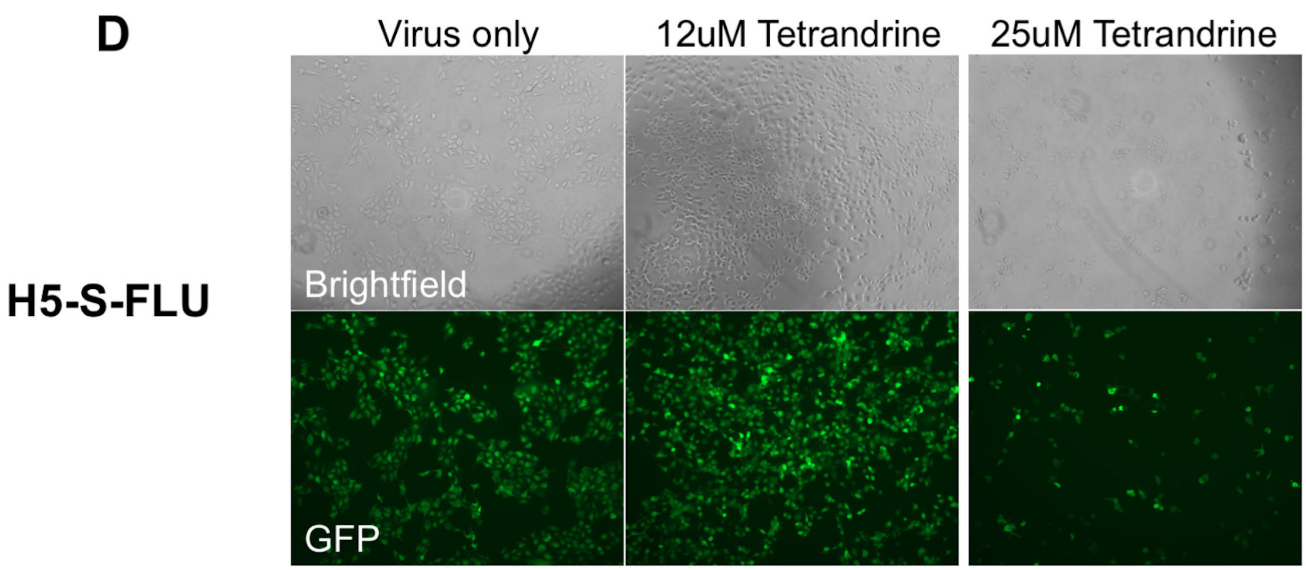
D
Virus only
12uM Tetrandrine
25uM Tetrandrine
H5-S-FLU
Brightfield
GFP

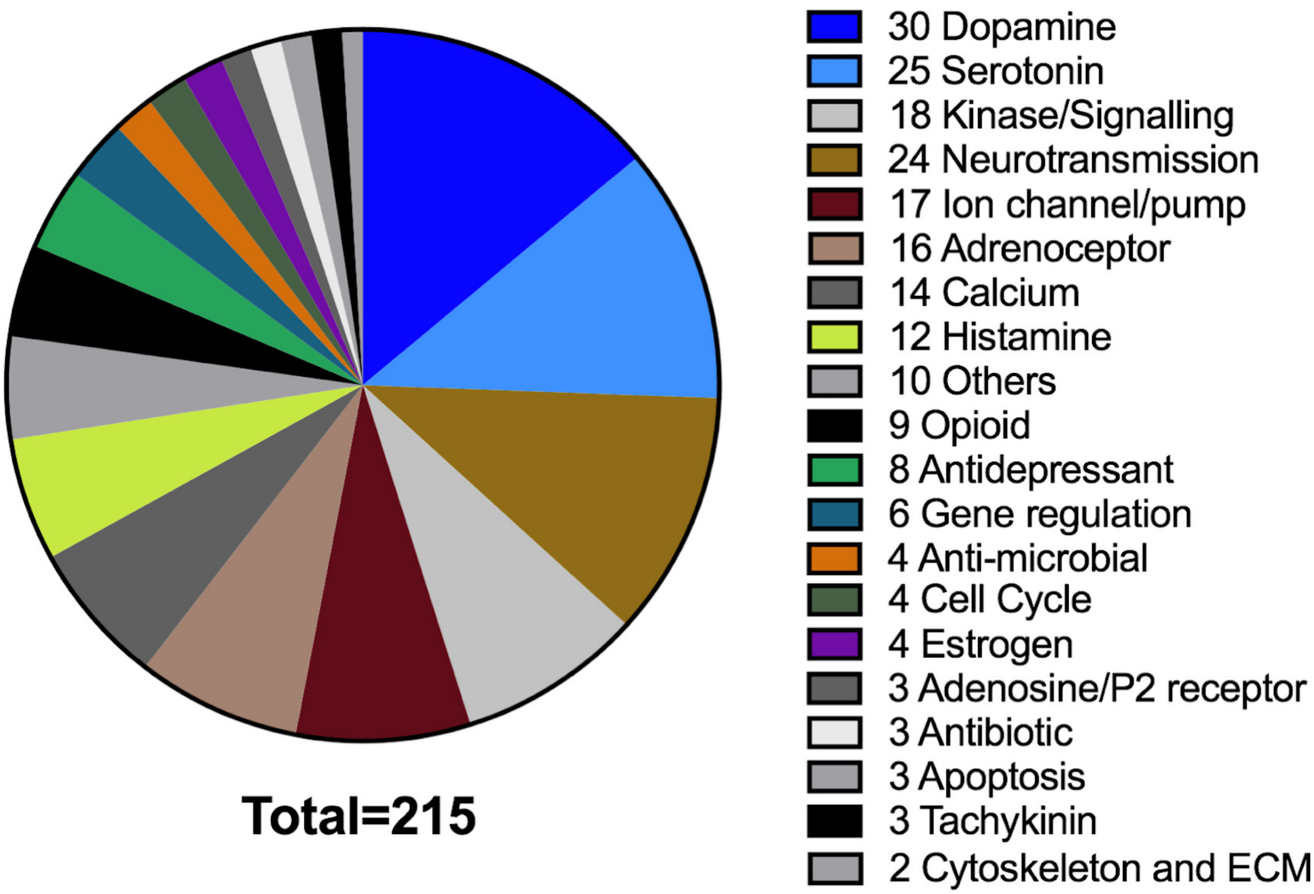
30 Dopamine
25 Serotonin
18 Kinase/Signalling
24 Neurotransmission
17 Ion channel/pump
16 Adrenoceptor
14 Calcium
12 Histamine
10 Others
9 Opioid
8 Antidepressant
6 Gene regulation
4 Anti-microbial
4 Cell Cycle
4 Estrogen
3 Adenosine/P2 receptor
3 Antibiotic
3 Apoptosis
3 Tachykinin
2 Cytoskeleton and ECM

Total=215

Journal of Virology

JVI

Journal of Virology

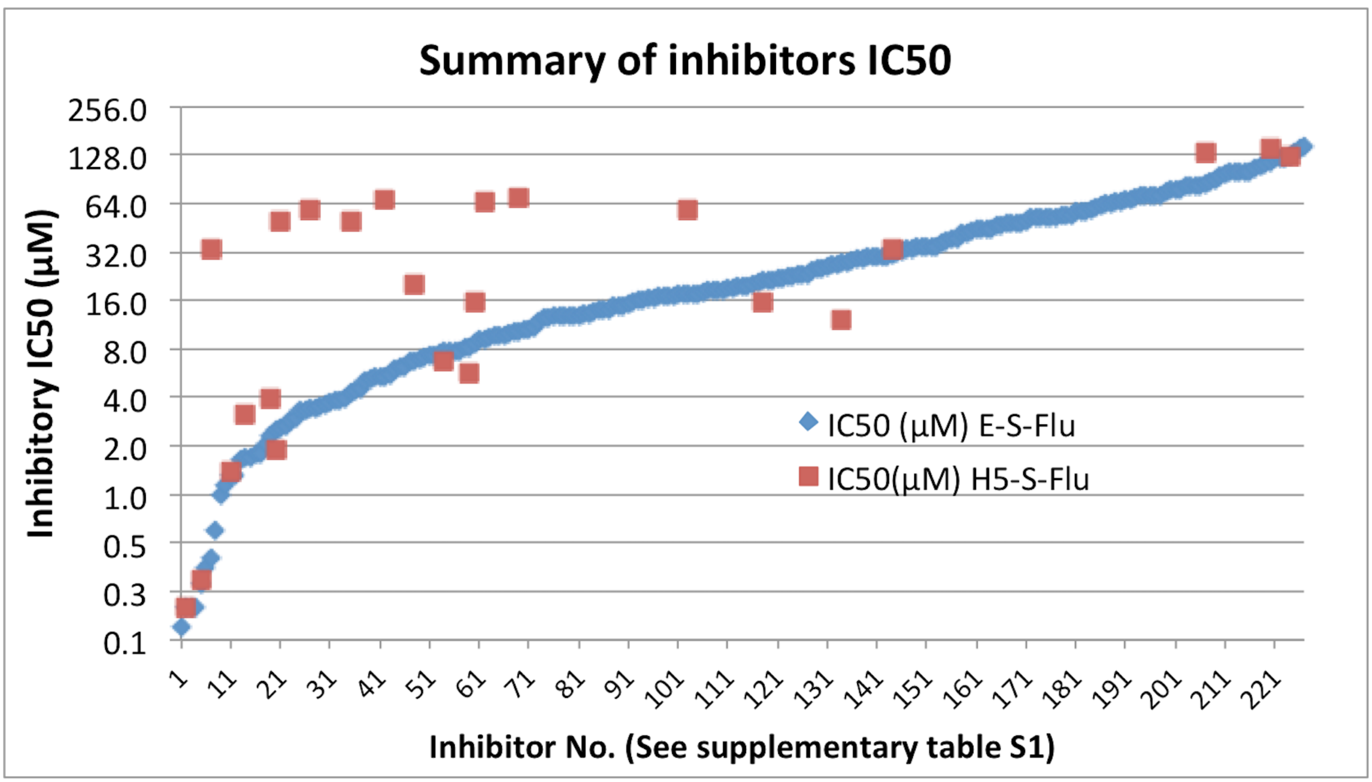

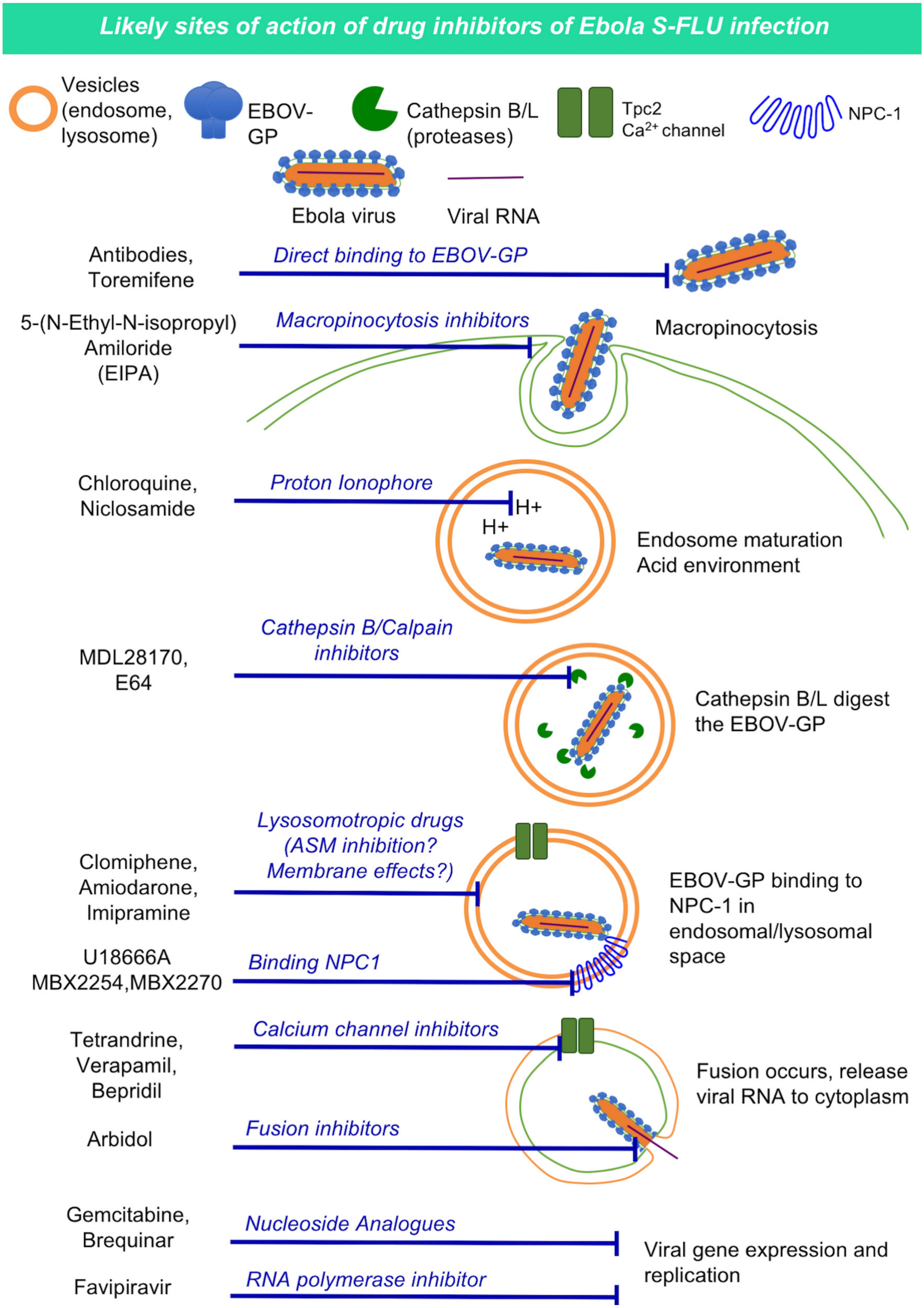
Likely sites of action of drug inhibitors of Ebola S-FLU infection
Vesicles (endosome, lysosome)
EBOV-GP
Cathepsin B/L (proteases)
Tpc2 Ca^{2+} channel
NPC-1
Ebola virus
Viral RNA
Antibodies, Toremifene
Direct binding to EBOV-GP
5-(N-Ethyl-N-isopropyl) Amiloride (EIPA)
Macropinocytosis inhibitors
Macropinocytosis
Chloroquine, Niclosamide
Proton Ionophore
H+
H+
Endosome maturation
Acid environment
MDL28170, E64
Cathepsin B/Calpain inhibitors
Cathepsin B/L digest the EBOV-GP
Clomiphene, Amiodarone, Imipramine
Lysosomotropic drugs (ASM inhibition? Membrane effects?)
U18666A MBX2254,MBX2270
Binding NPC1
EBOV-GP binding to NPC-1 in endosomal/lysosomal space
Tetrandrine, Verapamil, Bepridil
Calcium channel inhibitors
Arbidol
Fusion inhibitors
Fusion occurs, release viral RNA to cytoplasm
Gemcitabine, Brequinar
Nucleoside Analogues
Favipiravir
RNA polymerase inhibitor
Viral gene expression and replication